

AN ABSTRACT OF THE THESIS OF

Chang Chun Ma for the degree of Master of Science in

Nuclear Engineering presented on December 13, 1993

Title: Study of Interfacial Condensation in a Nuclear Reactor

Core Makeup Tank

Abstract Approved:

Redacted for Privacy

JR., Jose N. Reyes

Steam interfacial condensation in a core makeup tank was simulated using the code RELAP5/MOD3 version 8.0 to predict the violent pressure oscillation phenomena in a core makeup tank. Six base cases were carried out to study the effects of back pressure and of vacuum conditions produced in the core makeup tank by rapid steam condensation. The effect of varying the liquid conduction thermal layer thickness was studied. In addition, the code's ability to predict condensation heat transfer was evaluated.

Violent pressure oscillations were found in the early period of a transient. The violent pressure oscillations had no effect on the total amount of injection water from core makeup tank. The conduction thermal layer thickness was found to only effect the liquid temperature history. The current version of RELAP5/MOD3 was found to be incapable of dealing with the condensation heat transfer problem in which the volume liquid temperature is lower than the temperature of the heat structure which is connected to that hydraulic volume.

Study of Interfacial Condensation in a Nuclear Reactor Core Makeup Tank

by

Chang Chun Ma

A THESIS

submitted to

Oregon State University

in partial fulfillment of
the requirements for the
degree of

Master of Science

Completed December 13, 1993

Commencement June 1994

APPROVED:

Redacted for Privacy

Associate Professor of Nuclear Engineering in charge of major.

Redacted for Privacy

Head of Nuclear Engineering Department.

Redacted for Privacy

Dean of Graduate School.

Date thesis is presented December 13, 1993

Typed by Chang Chun Ma

ACKNOWLEDGEMENT

I want to dedicate this Master's degree to my parents for their moral and spiritual support. Their long-term plans have made this thesis possible.

I wish to thank Dr. JR., Jose N. Reyes, my major professor and advisor, who contributed significantly to my educational, scientific and personal development with his continual support and advice since the beginning of this research project.

I want to thank Dr. Mary M. Kulas, Mr. John T. Groome, and Dr. Abd Y. Lafi for their kind advice and support in using RELAP5. I would also like to thank Sandra M. Sloan, the worksheet ISBIM developer, for making the input deck preparation a lot easier. I should express my sincere gratitude to my friends, Hsing Hui Lee and Shahab Abdul-Hamid, for their help in my thesis writing.

Table of Contents

| | |
|--|----|
| 1. Introduction | 1 |
| 2. OSU AP600 Facility and Test Description | 4 |
| 2.1 Facility Description | 4 |
| 2.2 Test Description | 5 |
| 3. Code and Modelling Description | 7 |
| 3.1 Code Description | 7 |
| 3.2 Modelling Description | 13 |
| 4. Results and Discussion | 15 |
| 4.1 Base Case Discussion | 15 |
| 4.2 Conduction Thermal Layer Thickness Sensitivity Study | 17 |
| 4.3 Estimation of the Force Exerted on the CMT Tank | 18 |
| 4.4 Discussion of Code Limitation In Applying Condensation Model | 21 |
| 5. Conclusion | 23 |
| 6. References | 25 |
| Appendices | 61 |

List of Figures

| <u>Figure</u> | <u>Page</u> |
|---|-------------|
| 4.0 Control volume defined by the fluid surface in the CMT tank2.1 | 19 |
| 2.1 OSU AP600 test facility overall configuration | 33 |
| 2.2 Configuration of CMT tank steam condensation test facility | 34 |
| 3.1 Nodalization diagram for base case calculation | 35 |
| 4.1 Comparison of volume pressure among case 1, 2 and 3 | 36 |
| 4.2 Comparison of injection mass flow rate among case 1, 2 and 3 | 37 |
| 4.3 CMT tank vapor mass generation rate in case 1 | 38 |
| 4.4 CMT tank vapor mass generation rate in case 2 | 39 |
| 4.5 CMT tank vapor mass generation rate in case 3 | 40 |
| 4.6 CMT tank vapor void fraction changed with time in case 1 | 41 |
| 4.7 CMT tank vapor void fraction changed with time in case 2 | 42 |
| 4.8 CMT tank vapor void fraction changed with time in case 3 | 43 |
| 4.9 CMT tank liquid temperature changed with time in case 1 | 44 |
| 4.10 CMT tank liquid temperature changed with time in case 2 | 45 |
| 4.11 CMT tank liquid temperature changed with time in case 3 | 46 |
| 4.12 Comparison of CMT tank water level in case 1, 2 and 3 | 47 |
| 4.13 Comparison of CMT tank amount of water injected in case 1, 2 and 3 | 48 |
| 4.14 Comparison of CMT tank amount of water injected between case 1 and 4 | 49 |
| 4.15 Comparison of CMT tank amount of water injected between case 2 and 5 | 50 |
| 4.16 Comparison of CMT tank amount of water injected between case 3 and 6 | 51 |
| 4.17 Comparison of CMT tank injection mass flow rate between case 1 and 4 | 52 |
| 4.18 Comparison of CMT tank injection mass flow rate between case 2 and 5 | 53 |
| 4.19 Comparison of CMT tank injection mass flow rate between case 3 and 6 | 54 |
| 4.20 Comparison of CMT tank injection mass flow rate between case 2 and 7 | 55 |
| 4.21 Comparison of pressure in the CMT tank between case 2 and 7 | 56 |
| 4.22 Comparison of temperature in the 1st volume of the CMT tank between case 2 and case 7 | 57 |

| | | |
|------|---|----|
| 4.23 | Comparison of vapor mass generation rate in the 1st volume of the CMT tank between case 2 and case7 | 58 |
| 4.24 | Comparison of temperatures between liquid volume and its adjoining heat structure | 59 |
| 4.25 | Comparison of heat flux between hydraulic volume and its adjoining heat structure | 60 |

List of Tables

| <u>Table</u> | | <u>Page</u> |
|--------------|--|-------------|
| 3.1 | Summary of the important items in nodalization | 26 |
| 3.2 | Summary of the initial and boundary condition for case 1 | 27 |
| 3.3 | Summary of the initial and boundary condition for case 2 | 28 |
| 3.4 | Summary of the initial and boundary condition for case 3 | 29 |
| 3.5 | Summary of the initial and boundary condition for case 4 | 30 |
| 3.6 | Summary of the initial and boundary condition for case 5 | 31 |
| 3.7 | Summary of the initial and boundary condition for case 6 | 32 |

List of Appendices

| <u>Appendix</u> | <u>Page</u> |
|---|-------------|
| Appendix A. Natural Convective Heat Transfer Coefficient For The Outer Surface of The CMT tank (OSU Model) | 61 |
| Appendix B. RELAP5 Input Deck For The Model Without Heat Structure | 62 |
| Appendix C. RELAP5 Input Deck For The Model With Heat Structure | 69 |

Study of Interfacial Condensation in a Nuclear Reactor Core Makeup Tank

1. Introduction

After the lessons learned from the TMI and Chernobyl accidents, it has been widely thought that a new generation of PWR will have to incorporate step improvements in safety, reliability, as well as owner generation costs. The Advanced 600 MW PWR (AP600) developed by Westinghouse and supported by the US Department of Energy and EPRI provides significant improvements in these areas.

The AP600 is a two-loop pressurized water reactor. Each loop comprises one hot leg, two cold legs and one U-tube steam generator integrated with two canned motor coolant pumps. The significant difference is related to the passive nature of the safety and support systems of the AP600. This type of reactor is designed to increase the safety features that minimize negative consequences of human error and to introduce significant simplification in plant safety and non-safety systems and operation. The passive safety systems of the AP600 consist of two full pressure core make up tanks (CMT's), one In-containment Refueling Water Storage Tank (IRWST), a Passive Residual Heat Removal (PRHR) system with a heat exchanger submerged in the IRWST, two conventional accumulators and an Automatic Depressurization System (ADS), which consists of a set of valves located in the pressurizer steam zone and in one of the two hot legs.

In contrast with a conventional PWR plant, the AP600 plant features a low power density core and a passive safeguard system. Each steam generator and its pair of reactor coolant pumps are integrated into a single structure. Therefore the pump suction seal can be eliminated and thus the supporting structure is simplified. Moreover, the pressurizer in the AP600 has been enlarged to supply leakage make-up to better withstand transients. These most important improvements make the AP600 plant safer, simpler and more economic.

Oregon State University (OSU) is building the AP600 model in 1/4 scale. The OSU model will be used to test the AP600 long term cooling performance as well as some other integral system features. The test results will help the licensing evaluation process.

Computer simulation is also being performed to evaluate the AP600 long term cooling capability, which will be compared with experimental results later. RELAP5/MOD3[1], which is developed by the Idaho National Engineering Laboratory (INEL) under the sponsorship of the United States Nuclear Regulatory Commission, has frequently been used in the safety analysis of pressurized water reactors. This report is part of the RELAP5/MOD3 code simulation for OSU AP600 long term cooling phenomenon.

The core makeup tank is a new feature design in the AP600. In a Loss of Coolant Accident (LOCA), two CMT tanks will drain their contents into the reactor core through Direct Vessel Injection lines (DVI) by gravity after either a pressurizer low level or low pressure has been reached. Each CMT tank is connected to a cold

leg by a Pressure Balance Line (PBL). Thus the pressure in the CMT tank maintains the same pressure as in the reactor vessel. When the water level drops in the CMT tank, vapor is generated in the cold legs and is pressurized down into the CMT tanks through the PBL line. The rapid condensation on the steam/water interface causes pressure oscillations above the CMT water level. This results in the shaking of the CMT tank and may affect the amount of water injected by CMT tank as well. The amount of water injected into the reactor core is critical to mitigating LOCAs. In this report, the effect of rapid vapor condensation on the amount of water injected is studied by using RELAP5 to simulate the CMT tank draining process. The study will also evaluate the code capability in condensation heat transfer modelling.

The descriptions of the OSU test facility and the CMT tank rapid steam condensation test are provided in Chapter 2. The code and modelling for the CMT tank draining process are described in Chapter 3. The results and discussion are presented in Chapter 4, and general conclusions are drawn in Chapter 5.

2. OSU AP600 Facility and Test Description

2.1 Facility description

The OSU AP600 test facility is built to evaluate the thermal performance of the passive safety injection systems by generating system performance data. It is a scaled representation of the AP600 with a 1/4 length scale and a 1/2 time scale. The scaling analysis assures that the thermal hydraulic behavior in the OSU model is similar to that in the AP600. The test results will be used to license the AP600.

The OSU AP600 test facility includes the whole primary loop and emergency core cooling system. It consists of one reactor vessel, one pressurizer, two steam generators, four reactor coolant pumps, two hot legs, four cold legs, two core makeup tanks, two accumulators, one IRWST, one sump tank, one PRHR, two DVI injection lines, and an ADS system. The overall configuration is shown in Figure 2.1.

The entrance boundary is set on the secondary loop feed water supplies. The exit boundary is set immediately before the main steam line isolation valve. When an accident occurs, the main steam line isolation valve will be closed to isolate the secondary loop.

The OSU test facility is designed to operate at 700 kw power (electrically heated), 400 psia pressure, and 400 °F hot leg temperature.

Instead of modelling the whole OSU AP600 test facility to study CMT tank violent interfacial condensation during a LOCA, a simplified model, which sets the inlet boundary at the entrance of the PBL line and the outlet boundary at the exit of the DVI line, is utilized. The inlet boundary is modeled by a steam supply tank substituted for the reactor vessel generating steam. The outlet boundary is modeled by a sump tank used to specify the back pressure. The simplified model for studying CMT tank violent steam condensation consists of a CMT tank, a PBL line, a CMT injection line, and a DVI line. All these components are physically the same as those in the OSU AP600 test facility. The pressure drop for each component is also modeled. The test facility modeled using RELAP5 is shown in Figure 2.2.

2.2 Test description

The purpose of the test is to examine the effect of rapid condensation of vapor in the CMT tank, which may cause the shaking of the CMT tank and water injection rate oscillation.

Prior to the experiment, the CMT tank is filled with subcooled water at a pressure of 400 psia and a temperature of 100 °F. The CMT injection line, and DVI line are also filled with subcooled water at the same pressure and temperature. Both PBL line and steam supply tank are filled with saturated steam at a pressure of 400 psia. The CMT tank is isolated from both the PBL line and the CMT injection line by closing the isolation valves on the top and the bottom of the CMT tank, respectively.

Another valve is deployed to isolate the CMT injection line from the DVI line to prevent motion caused by gravity.

The experiment is initiated by opening all the Quick-Opening valves in the test facility. The CMT tank starts to inject coolant by gravity. Steam condenses on both the liquid and the CMT tank inside wall surface. The rapid condensation results in an instant vacuum condition in the volume above the steam/water interface. Then the saturated steam rushes into that volume. This condensation and instant vacuum condition occurs repeatedly.

3. Code and Modelling Description

3.1 Code Description

The RELAP5/MOD3 code is the third major variant of the RELAP5 advanced thermal-hydraulic code that was originally released by Idaho National Engineering Laboratory (INEL) in 1979. It was originally designed to analyze complex thermal-hydraulic interactions that occur during either postulated large break or small break loss of coolant accidents in PWRs. However, as development continued, the code was expanded to include many of the transient scenarios that might occur in thermal-hydraulic systems. The code has been successfully used to analyze not only large and small break LOCAs, but also operational transients in conventional PWRs. The code could also be used for boiling water reactor system analysis.

Hydrodynamic Model The RELAP5 hydrodynamic model is a one-dimensional, transient, two-fluid model for the flow of a two-phase steam-water mixture that can contain noncondensable components in the steam phase and/or a nonvolatile component in the water phase. The two-fluid nonequilibrium hydrodynamic model includes options for simpler hydrodynamic models. Included are a homogeneous flow model and/or a thermal equilibrium model. The two-fluid or homogeneous flow models can be used with either the nonequilibrium or equilibrium thermal models, i.e., four combinations.

Field Equations RELAP5 solves six basic field equations for six primary dependent variables. The six primary dependent variables are pressure (P), phase-specific internal energies (U_g, U_f), vapor void fraction (α_g), and phasic velocities (v_g, v_f). The independent variables are time (t) and distance (x). The six basic field equations for the two-fluid nonequilibrium model consist of two-phasic continuity equations, two-phasic momentum equations, and two-phasic energy equations.

The phasic mass conservation equations[2] are

$$\frac{1}{V} \frac{\partial}{\partial t}(V \alpha_g \rho_g) + \frac{1}{A} \frac{\partial}{\partial x}(\alpha_g \rho_g v_g A) = \Gamma_g \quad (3-1)$$

$$\frac{1}{V} \frac{\partial}{\partial t}(V \alpha_f \rho_f) + \frac{1}{A} \frac{\partial}{\partial x}(\alpha_f \rho_f v_f A) = -\Gamma_g \quad (3-2)$$

The phasic momentum equations[2] are

$$\begin{aligned} \alpha_g \rho_g A \frac{\partial v_g}{\partial t} + \frac{1}{2} \alpha_g \rho_g A \frac{\partial v_g^2}{\partial x} = & -\alpha_g A \frac{\partial P}{\partial x} + \alpha_g \rho_g B_x A - (\alpha_g \rho_g A) FWG(v_g) \\ & + \Gamma_g A (v_{gl} - v_g) - (\alpha_g \rho_g A) FIG(C_1 v_g - C_0 v_f) + f_{\tau g} A |v_g| v_g \\ & - f_{\tau f} A |v_f| v_f - C \alpha_g \alpha_f \rho A \left[\frac{\partial(v_g - v_f)}{\partial t} + v_f \frac{\partial v_g}{\partial x} - v_g \frac{\partial v_f}{\partial x} \right] \end{aligned} \quad (3-3)$$

$$\begin{aligned}
\alpha_f \rho_f A \frac{\partial v_f}{\partial t} + \frac{1}{2} \alpha_f \rho_f A \frac{\partial v_f^2}{\partial x} &= -\alpha_f A \frac{\partial P}{\partial x} + \alpha_f \rho_f B_x A - (\alpha_f \rho_f A) \text{FWG}(v_f) \\
- \Gamma_g A (v_{fl} - v_f) - (\alpha_f \rho_f A) \text{FIG}(C_0 v_f - C_1 v_g) + f_{\tau f} A |v_f| v_f \\
- f_{\tau g} A |v_g| v_g - C \alpha_f \alpha_g \rho A \left[\frac{\partial(v_f - v_g)}{\partial t} + v_g \frac{\partial v_f}{\partial x} - v_f \frac{\partial v_g}{\partial x} \right]
\end{aligned} \tag{3-4}$$

The phasic energy equations[2] are

$$\begin{aligned}
\frac{\partial}{\partial t}(\alpha_g \rho_g U_g) + \frac{1}{A} \frac{\partial}{\partial x}(\alpha_g \rho_g U_g v_g A) &= -P \frac{\partial \alpha_g}{\partial t} - \frac{P}{A} \frac{\partial}{\partial x}(\alpha_g v_g A) \\
+ Q_{wg} + Q_{ig} + \Gamma_{ig} h_g^* + \Gamma_w h_g^s + \text{DISS}_g
\end{aligned} \tag{3-5}$$

$$\begin{aligned}
\frac{\partial}{\partial t}(\alpha_f \rho_f U_f) + \frac{1}{A} \frac{\partial}{\partial x}(\alpha_f \rho_f U_f v_f A) &= -P \frac{\partial \alpha_f}{\partial t} - \frac{P}{A} \frac{\partial}{\partial x}(\alpha_f v_f A) \\
+ Q_{wf} + Q_{if} + \Gamma_{if} h_f^* + \Gamma_w h_f^s + \text{DISS}_f
\end{aligned} \tag{3-6}$$

If a noncondensable phase (i.e. air) exists, it adds an additional mass conservation equation for the total noncondensable component, given by

$$\frac{1}{V} \frac{\partial}{\partial t} (V \alpha_g \rho_g X_n) + \frac{1}{A} \frac{\partial}{\partial x} (\alpha_g \rho_g X_n v_g A) = \sum_{ni=1}^N \Gamma_{ni}$$

(3-7)

State relationships The six-equation model with an additional equation for the noncondensable gas component has five independent state variables. The independent variables are chosen to be P , α_g , U_g , U_f , and X_n . All the remaining thermodynamic variables (temperatures, densities, partial pressures, qualities, etc.) are expressed as functions of these five independent properties.

In addition to the state properties, derivatives of the mixture density with respect to the pressure, static quality, and mixture internal energy are required in the numerical solution scheme. These derivatives can be expressed in terms of the isothermal compressibility (κ), the isobaric coefficient of thermal expansion coefficient (β), and the specific heat at constant pressure (C_p), all of which are available from the state properties data.

Constitutive Relations The constitutive relations include models for defining flow regimes and flow-regime-related models for interphase drag and shear, the coefficient of virtual mass, wall friction, wall heat transfer, and interphase heat and mass transfer. There are four constitutive relations required by the hydrodynamic model--the vapor generation rate, the interphase drag, the wall friction, and the wall heat transfer.

Numerical Methods The RELAP5 numerical solution scheme is based on replacing the system of differential equations with a system of finite difference equations, which are partially implicit in time. A physical system consisting of flow paths, volumes, areas, etc., is simulated by constructing a network of control volumes connected by junctions. The hydrodynamic model and the associated numerical scheme are based on the use of fluid control volumes and junctions to represent the spatial character of the flow. It is a one-dimensional model of the transient flow of a steam-water-noncondensable mixture. The control volumes can be viewed as stream tubes having inlet and outlet junctions. The control volume has a direction associated with it that is positive from the inlet to the outlet. The fluid scalar properties, such as pressure, energy, density, and void fraction, are represented by the average fluid conditions and are viewed as being located at the control volume center. The fluid vector properties, such as velocities, are located at the junctions and are associated with mass and energy flow between control volumes. Control volumes are connected in series using junctions to represent a flow path.

Heat Structure and other special models Heat flow paths are also modeled in a one-dimensional sense using a staggered mesh to calculate temperatures and heat flux vectors. The heat conductors can be connected to hydrodynamic volumes to simulate a heat flow path normal to the fluid flow path. The heat conductor or heat structure is thermally connected to the hydrodynamic volume through a heat flux that is calculated using a boiling heat transfer formulation. The heat structures are used to simulate pipe walls, heater elements, nuclear fuel pins, and heat exchanger surfaces.

The interface mass transfer is modeled according to the volume flow regime. For the general bulk mass transfer processes, the interfacial mass transfer model in the bulk fluid depends on the volume flow regime. In the bubbly flow regime, for the liquid side, interfacial mass transfer is the larger of either the model for bubble growth developed by Plesset and Zwick[3] or the model for convective heat transfer for a spherical bubble (modified Lee and Ryley)[4]. For the vapor side, an interphase heat transfer coefficient is assumed that is high enough to drive the vapor temperature toward saturation. Analogously, in the mist regime, for the vapor side, a convective heat transfer model for a spherical droplet is used for the interphase heat transfer coefficient. For the liquid side, an interphase heat transfer coefficient is assumed that is high enough to drive the liquid temperature toward saturation. For condensation process, the interfacial mass transfer in the bulk fluid, for the liquid side, is calculated by the Unal bubble collapse model[5] in the bubbly flow regime and by the Brown droplet model[6] and the Theofanous interfacial condensation model[7] in the annular mist flow regime. For the vapor side, a large interphase heat transfer coefficient is assumed in order to drive the vapor temperature toward saturation.

Extensive trip logic has been implemented in RELAP5. The trip logic is designed to determine when a certain trip has occurred. Trip capability provides for variable and logical trips. With the capabilities of trip component and control variable component, RELAP5 is able to simulate the transient of systems and components.

3.2 Modelling Description

The nodalization scheme selected for the components in this test study is basically the same as that proposed for the OSU AP600 model except for the CMT tank. In the OSU AP600 model, the CMT tank is modeled by two components. The top hemispherical part is modeled by a component branch with two junctions. The rest is modeled by a component pipe with eight subvolumes. Because of code limitations, the nodalization scheme of the CMT tank in the OSU AP600 model is not complete. Currently axial conduction heat transfer through the water can not be modeled in RELAP5. The fluid temperature in the hydraulic volume can only be changed through interfacial mass transfer or by fluid motion. However the heat transfer by conduction through the water is significant in the test. To best include the effect of conduction heat transfer through the water, the length of the first volume in CMT tank is determined by the thermal layer of conductive heat transfer. The estimation of the thermal layer length is included in Appendix A.

The inlet flow boundary is specified by using a single volume component for the steam supply tank, coupled with a single junction component connecting the steam supply tank to the PBL line. The reason why the inlet flow boundary condition is not specified by connecting a time dependent volume and a time dependent junction at the end of a PBL line is that the steam mass flow rate is not constant. In reality, it is determined by the pressure difference between the pressure in the steam supply tank and the pressure in the CMT tank.

The outlet pressure boundary is specified by using a time dependent volume component for the sump tank and a single junction component connected to the end of the DVI line. The outlet time dependent volume specifies a constant back pressure.

The important items of the nodalization scheme are shown in Table 3.1. The overall nodalization diagram is shown in Figure 3.1.

Six base cases are calculated in this report. Case 1, 2 and 3 which have different back pressure are designed to examine the effects of the back pressures. Case 4, 5 and 6 are case 1, 2 and 3 respectively except the PBL line and the steam supply tank are filled with air instead of steam. The purpose of this study is to examine the effects of the steam condensation. The descriptions of each of these cases are given in tables. Table 3.2 to Table 3.7 summarize the initial and boundary conditions along with the other information for each of these cases. The wall heat structure of the CMT tank is not modeled in the base cases. The model with the heat structure is provided to evaluate the code's capability of dealing with the wall condensation heat transfer problem. Another calculation using a different length for the first volume of the CMT tank is also presented to study the effects of the thermal layer thickness. The input deck for each case is presented in Appendix B. All the component inputs were prepared on a Macintosh using a Claris Resolve software package. The simulation has been performed on an HP730 workstation.

4. Results and Discussion

The six base transient calculations are presented in this chapter. The transient is simulated for a time period of 900 seconds. The results of the transients up to 450 seconds are summarized by plots, during which the CMT tank completely drains at about 400 seconds for case 1 and case 4, 160 seconds for case 2 and case 5, 75 seconds for case 3 and case 6. Case 7 provides a conduction thermal layer sensitivity study. The discussion of the code's limitation in dealing with the condensation heat transfer problem is also presented in this chapter.

4.1 Base case discussion

The CMT pressure behaviors in cases 1, 2 and 3 are shown in Figure 4.1. During the first 100 seconds, violent pressure oscillations are observed in case 2; minor pressure oscillations are shown in case 3. In case 1, the pressure remains almost constant. The pressure oscillation is caused by rapid steam condensation on the subcooled liquid surface which results in an instant vacuum condition in the CMT tank. It is also affected by the void fraction in the CMT tank. In case 2 and case 3, the back pressure in the boundary volume is lower than the vapor saturation pressure. This is the reason why violent steam condensation is observed in case 2 and case 3 but not in case 1, where the back pressure in the boundary volume is the same as the vapor saturation pressure (see Figure 4.3, Figure 4.4, and Figure 4.5). As mentioned

previously, whether the rapid steam condensation on the steam/liquid interface would affect the volume pressure significantly is determined by the vapor void fraction in the CMT tank. If the CMT tank has enough vapor volume, the small amount of vapor condensed on the steam/liquid interface will not affect the total volume pressure. As shown in Figure 4.1, after the first 100 seconds, when most of the volume in the CMT tank has been filled with steam, the volume pressure in case 2 and case 3 tend to be constant.

It is also noticed from Figure 4.1 that the pressure oscillation in case 2 is more violent than the pressure oscillation in case 3. The violent pressure oscillation in case 2 is due to the reverse flow occurring as shown in Figure 4.2. The rapid steam condensation results in a vacuum condition in the CMT tank. When the difference between the pressure in the CMT tank and the pressure in CMT tank injection line is high enough to overcome the gravity, reverse injection flow occurs. The reverse flow decreases the vapor volume as shown in Figure 4.7, therefore it increases the effect of the vacuum condition caused by steam condensation.

The vapor void fractions in case 1 and case 3 always increase with time as shown in Figure 4.6 and Figure 4.8. The CMT tank liquid temperature smoothly increases in case 1 as shown in Figure 4.9. The liquid temperature jump in case 3 as shown in Figure 4.11 is caused by the oscillating injection mass flow rate. The big liquid temperature oscillation in case 2 is observed in Figure 4.10.

Figure 4.12 presents the comparison of CMT tank water level among case 1, case 2, and case 3. Again the oscillation of water level in the CMT tank is observed

in case 2. It is also noticed from Figure 4.12 that the lower the back pressure, the faster the water level goes down. Figure 4.13 compares the total amount of water injected among case 1, case 2 and case 3. It shows that the total amount of injection water is related to the back pressure. The lower the back pressure, the greater the amount of water injected.

Figure 4.15, Figure 4.16 and Figure 4.17 compare the total amount of water injected for the cases in which either steam or air is supplied. The purpose of this comparison is to study the effect of vapor condensation on the CMT tank total amount of injection water. Figure 4.15, Figure 4.16, and Figure 4.17 indicate that the vapor condensation does not affect the total amount of injection water in all three cases. The rapid vapor condensation does affect the injection mass flow rate (see Figure 4.17, Figure 4.18, and Figure 4.19).

4.2 Conduction thermal layer thickness sensitivity study

As mentioned in chapter 3, the length of the first volume in the CMT tank is determined by the conduction thermal layer thickness. The conduction thermal layer thickness δ is affected by the transient time. It is evaluated according to the following equation[8]:

$$\delta = \sqrt{8\alpha t} \tag{4-1}$$

where α is thermal diffusivity and t is transient time.

In the base case calculation, the transient time used to determine the conduction thermal layer thickness is 400 seconds, during which the CMT tank has completely drained. The corresponding length of the first volume in the CMT tank is 2.5177 feet. In case 7, the transient time used to calculate the conduction thermal layer thickness is chosen to be 300 seconds. The corresponding length of the first volume in the CMT tank is 2.18 feet. The rest of the nodalization scheme, initial condition, and boundary condition in case 7 are the same as those in case 2.

Figure 4.20, Figure 4.21, and Figure 4.23 show that the vapor mass generation, the volume pressure, and the injection mass flow rate are not sensitive to the conduction thermal layer. But the liquid temperature in the CMT tank is very sensitive to the conduction thermal layer as shown in Figure 4.22. The big liquid temperature oscillation in case 2 does not occur in case 7, while the only difference between case 2 and case 7 is the conduction thermal layer.

4.3 Estimation of the force exerted on the CMT tank

The force exerted on the CMT tank by the liquid has the same magnitude as the force imposed on the liquid by the CMT tank. To estimate the force exerted on the CMT tank, we choose all liquid in the CMT tank as a control volume and apply the conservation momentum equation to this control volume. The control volume chosen in this manner is designated in Figure 4.0, showing the external forces imposed upon it. The external forces imposed on the fluid include the pressure forces P_1 and P_2

at the sections (1) and (2), the body force due to the weight of fluid in the control volume, W , and the force exerted on the fluid by the CMT wall, F .

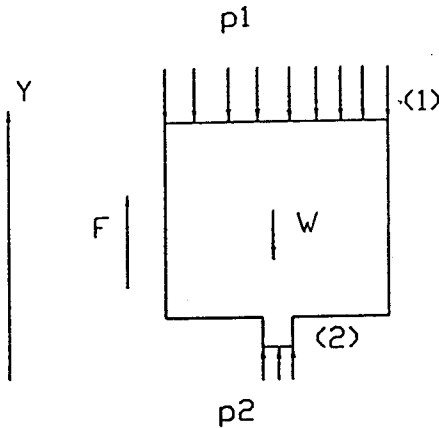


Figure 4.0 Control volume defined by the fluid surface in the CMT tank

Considering the conservation momentum equation in the y direction and noticing that, for the normal operation, the fluid velocity is negative in the y direction; for the reverse situation, the fluid velocity is positive in the y direction, and the external forces acting on the fluid in the control volume are

$$\Sigma F_y = P_2 A_2 - P_1 A_1 + F - W \quad (4-2)$$

The net rate of momentum afflux from the control volume is

for the normal operation

$$\iint_{c.s.} v \rho (v \cdot n) dA = v_2^2 \rho A_2 - v_1^2 \rho A_1 \quad (4-3)$$

and for the reverse situation

$$\iint_{c.s.} \mathbf{v} \rho (\mathbf{v} \cdot \mathbf{n}) dA = -v_2^2 \rho A_2 + v_1^2 \rho A_1 \quad (4-4)$$

The accumulation term is assumed to be zero. Thus the force exerted on the fluid volume can be expressed as

$$F = v_2^2 \rho A_2 - v_1^2 \rho A_1 + P_1 A_1 - P_2 A_2 + W \quad \text{for the normal operation} \quad (4-5)$$

$$F = -v_2^2 \rho A_2 + v_1^2 \rho A_1 + P_1 A_1 - P_2 A_2 + W \quad \text{for the reverse flow} \quad (4-6)$$

The first two terms in the equations (4-5) and (4-6) are so small compared with the pressure force and the gravity force in this problem, that we can neglect their effects. Also we noticed that the back pressure P_2 , area A_1 and A_2 , are constant. Therefore the primary causes for the oscillation of the reaction force exerted on the CMT tank by the fluid are the pressure oscillation due to the violent steam condensation and the water level oscillation due to the reverse flow. In case 2, A_1 is 2.5349 ft², A_2 is 0.0068 ft², P_2 is 380 psia; before the reverse flow occurs, P_1 is 400 psia, the water height in the CMT tank is 1.6 feet; when the reverse flow occurs, P_1 drops to 74 psia, the water level in the CMT tank rises to 2.1759 feet. The calculation shows that the corresponding reaction force exerted on the CMT tank could oscillate between 153,182 lbf and 37,357 lbf when the oscillation flow occurs. This results in the CMT tank

shaking violently.

4.4 Discussion of code limitation in applying condensation model

Case 8 is provided to evaluate the code's capability in dealing with the condensation heat transfer problem. Based on case 1, the wall heat structure of the CMT tank is considered in case 8.

The heat structure boundary condition for the inside wall surface is specified as a convection boundary condition. The heat transfer boundary condition for the outside wall surface is specified as natural convective heat transfer. The heat transfer coefficient for natural convection and the sink temperature are defined by tables in the RELAP5 input deck. The calculation of the natural convective heat transfer coefficient is provided in Appendix A. The RELAP5 input deck for case 8 is attached in Appendix C.

The heat transfer to the liquid phase is the difference between the total heat transfer into the volume and the heat transfer into the vapor phase. In Figure 4.25, the value of heat transfer to the liquid phase is always negative; this means the heat flow path is from liquid to heat structure. This contradicts the results from Figure 4.24, which indicate the liquid temperature is lower than the surface temperature of its adjoining heat structure.

The contradiction is caused by the code limitation in dealing with the condensation problem. In the current RELAP5/MOD3 version 8.0, the logic control of

the condensation heat transfer mode is the vapor void fraction and the wall surface temperature. If the vapor void fraction is greater than 0.001 and less than 0.99, and if the wall surface temperature is below the saturation temperature, the condensation model is actuated[9]. In the condensation mode, the volume liquid temperature is always assumed to be greater than the surface temperature of its adjoining heat structure. This assumption is not mentioned in the RELAP5 manual, but was confirmed by Mr. Rex Shumway, who is in charge of developing RELAP5 condensation heat transfer model at Idaho National Engineering Laboratory[10].

In the future, the CMT wall heat structure will be used in modelling the CMT tank rapid steam condensation if the new RELAP5 version is capable of dealing with negative heat transfer.

5. Conclusions

RELAP5/MOD3 version 8.0 was used to simulate the steam condensation in the OSU AP600 CMT tank. Six base case calculations were carried out to study the effects of back pressure and violent steam condensation on the CMT injection mass flow rate. To determine the effect of the liquid conduction thermal layer depth on the CMT transient behavior, a seventh case, using a different conduction thermal layer thickness from that used in the base cases, was tested. In addition, the code capability in dealing with condensation heat transfer problems was evaluated by case 8. As a result of the present calculations, the following conclusions are obtained.

- 1) Violent pressure oscillations in the CMT tank occur in the early period of the transient. They are caused by the rapid vapor condensation on the steam/liquid interface.
- 2) Violent oscillations of the pressure and the water level in the CMT tank result in the oscillation of the force exerted on the CMT tank by the fluid, which causes the CMT tank shaking violently.
- 3) Rapid steam condensation could result in CMT tank shaking, but it does not affect the total amount of CMT water injected.
- 4) The total amount of CMT water injected is determined by the CMT tank back pressure; the lower the back pressure, the larger the amount of water injected.
- 5) CMT tank hydraulic behaviors such as volume pressure, injection mass flow rate, etc., are not sensitive to the conduction thermal layer. However, the

thickness of the conduction thermal layer is significant to the history of liquid temperature.

- 6) RELAP5/MOD3 version 8.0 has a limitation in the condensation heat transfer model. The model works well for the case in which the liquid temperature is higher than the wall inside surface temperature. However, when the liquid temperature is lower than the wall surface temperature, an unrealistic heat transfer path from liquid to wall is found.

6. References

1. K. E. Carlson, R. A. Riemke, et. al. "RELAP5/MOD3 Code Manual", NUREG/CR-5535, EGG-2596, Idaho National Engineering Laboratory, June 1990.
2. K. E. Carlson, R. A. Riemke, et. al. "RELAP5/MOD3 Code Manual", Volume 1, pp. 3.1-8, NUREG/CR-5535, EGG-2596, Idaho National Engineering Laboratory, June 1990.
3. M. S. Plesset and S. A. Zwick, "Growth of Vapor Bubbles in Superheated Liquids," Journal of Applied Physics, 25, 4, 1954, 493-500.
4. F. Kreith, "Principles of Heat Transfer", New York: Intext Press, Inc., 1973.
5. H. C. Unal, "Maximum Bubble Diameter, Maximum Bubble-Growth Time and Bubble-Growth Rate During the Subcooled Nucleate Flow Boiling of Water Up to 17. MN/m²", International Journal of Heat Mass Transfer, 19, 1976, pp. 643-649.
6. G. Brown, "Heat Transmission by Condensation on a Spray of Water Drops," Institute of Mechanical Engineers, 1951, pp. 49-52.
7. T. G. Theofanous, "Modeling of Basic Condensation Processes," The Water Reactor Safety Research Workshop on Condensation, Silver Springs, MD, May 24-25, 1979.
8. M. Necati Ozisik, "Heat Conduction", pp. 336, JOHN WILEY&SONS, 1980.
9. K. E. Carlson, R. A. Riemke, et. al. "RELAP5/MOD3 Code Manual", Volume 1, pp. 3.3-60, NUREG/CR-5535, EGG-2596, Idaho National Engineering Laboratory, June 1990.
10. R. Shumway, EG&G Idaho, Inc., Private Communication (1993).
11. A. Parrish, "Mechanical Engineering's Reference Book 11th Edition", BUTTERWORTHS, 1980.

Table 3.1 Summary of the important items in nodalization

| items | component type (number) | volumes of componet |
|---------------------------------|-----------------------------|---------------------|
| steam tank | single volume (900) | 1 |
| PBL line (part 1) | pipe (857) | 7 |
| PBL line (part 2) | pipe (858) | 5 |
| CMT tank top isolation valve | valve (859) | 1 |
| CMT tank | pipe (860) | 3 |
| CMT tank bottom isolation valve | valve (861) | 1 |
| CMT tank surge line | pipe (862) | 2 |
| DVI isolation valve | valve (863) | 1 |
| DVI line | pipe (864) | 4 |
| sump tank | time dependent volume (915) | 1 |

Table 3.2 Summary of the initial and boundary conditions for case 1

| items | temperature (°F) | pressure (psia) | water/steam/air |
|---------------------|------------------|-----------------|-----------------|
| steam tank | saturated | 400.00 | steam |
| PBL line (part 1) | saturated | 400.00 | steam |
| PBL line (part 2) | saturated | 400.00 | steam |
| CMT tank | 100.00 | 400.00 | water |
| CMT tank surge line | 100.00 | 400.00 | water |
| DVI line | 100.00 | 400.00 | water |
| sump tank | 100.00 | 400.00 | water |

Note: Initial velocities at junctions are all zero.

Table 3.3 Summary of the initial and boundary conditions for case 2

| items | temperature (°F) | pressure (psia) | water/steam/air |
|---------------------|------------------|-----------------|-----------------|
| steam tank | saturated | 400.00 | steam |
| PBL line (part 1) | saturated | 400.00 | steam |
| PBL line (part 2) | saturated | 400.00 | steam |
| CMT tank | 100.00 | 400.00 | water |
| CMT tank surge line | 100.00 | 400.00 | water |
| DVI line | 100.00 | 400.00 | water |
| sump tank | 100.00 | 380.00 | water |

Note: Initial velocities at junctions are all zero.

Table 3.4 Summary of the initial and boundary conditions for case 3

| items | temperature (°F) | pressure (psia) | water/steam/air |
|---------------------|------------------|-----------------|-----------------|
| steam tank | saturated | 400.00 | steam |
| PBL line (part 1) | saturated | 400.00 | steam |
| PBL line (part 2) | saturated | 400.00 | steam |
| CMT tank | 100.00 | 400.00 | water |
| CMT tank surge line | 100.00 | 400.00 | water |
| DVI line | 100.00 | 400.00 | water |
| sump tank | 100.00 | 350.00 | water |

Note: Initial velocities at junctions are all zero.

Table 3.5 Summary of the initial and boundary conditions for case 4

| items | temperature (°F) | pressure (psia) | water/steam/air |
|---------------------|------------------|-----------------|-----------------|
| steam tank | saturated | 400.00 | air |
| PBL line (part 1) | saturated | 400.00 | air |
| PBL line (part 2) | saturated | 400.00 | air |
| CMT tank | 100.00 | 400.00 | water |
| CMT tank surge line | 100.00 | 400.00 | water |
| DVI line | 100.00 | 400.00 | water |
| sump tank | 100.00 | 400.00 | water |

Note: Initial velocities at junctions are all zero.

Table 3.6 Summary of the initial and boundary conditions for case 5

| items | temperature (°F) | pressure (psia) | water/steam/air |
|---------------------|------------------|-----------------|-----------------|
| steam tank | saturated | 400.00 | air |
| PBL line (part 1) | saturated | 400.00 | air |
| PBL line (part 2) | saturated | 400.00 | air |
| CMT tank | 100.00 | 400.00 | water |
| CMT tank surge line | 100.00 | 400.00 | water |
| DVI line | 100.00 | 400.00 | water |
| sump tank | 100.00 | 380.00 | water |

Note: Initial velocities at junctions are all zero.

Table 3.7 Summary of the initial and boundary conditions for case 6

| items | temperature (°F) | pressure (psia) | water/steam/air |
|---------------------|------------------|-----------------|-----------------|
| steam tank | saturated | 400.00 | air |
| PBL line (part 1) | saturated | 400.00 | air |
| PBL line (part 2) | saturated | 400.00 | air |
| CMT tank | 100.00 | 400.00 | water |
| CMT tank surge line | 100.00 | 400.00 | water |
| DVI line | 100.00 | 400.00 | water |
| sump tank | 100.00 | 350.00 | water |

Note: Initial velocities at junctions are all zero.

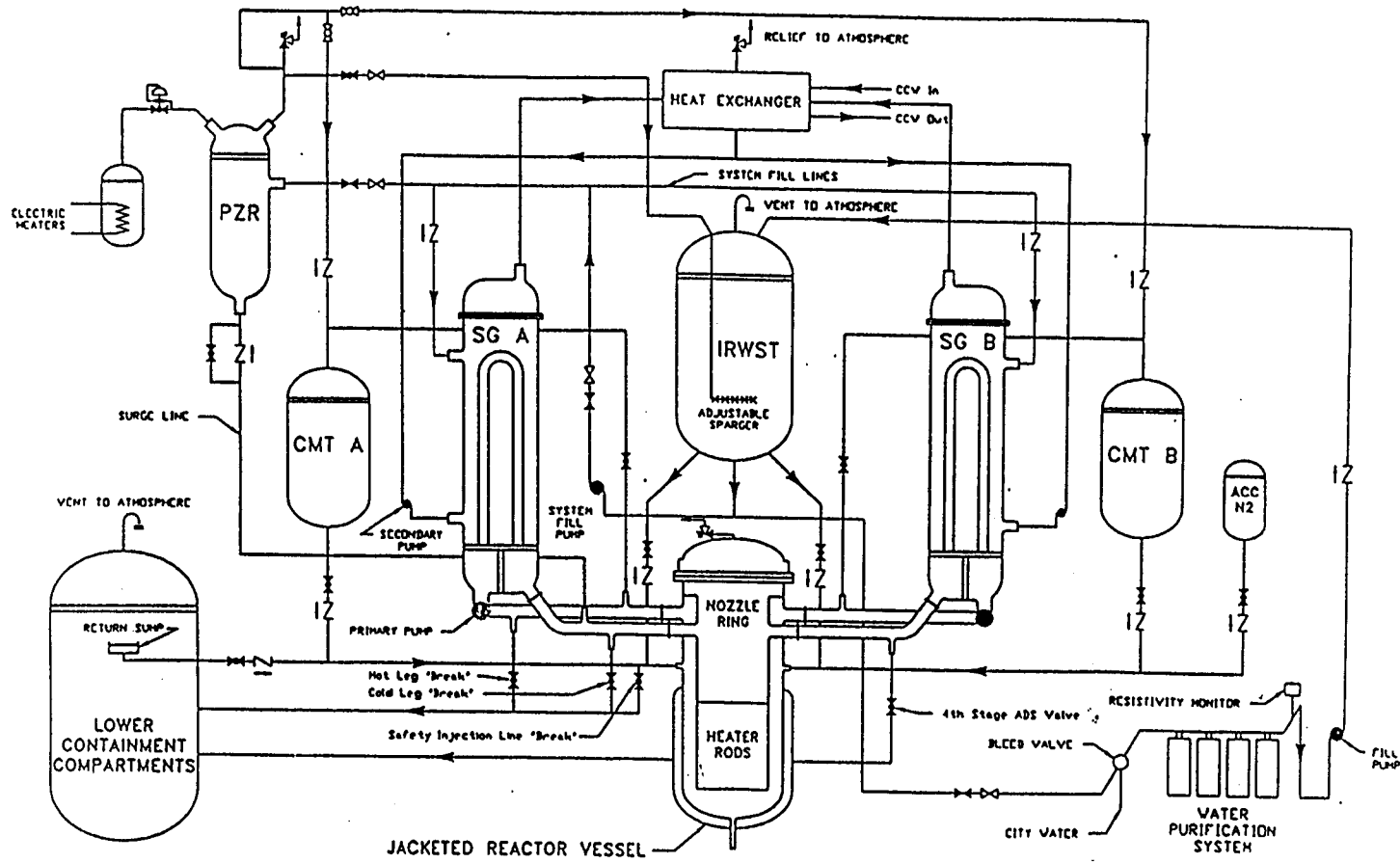


Figure 2.1 OSU AP600 test facility overall configuration

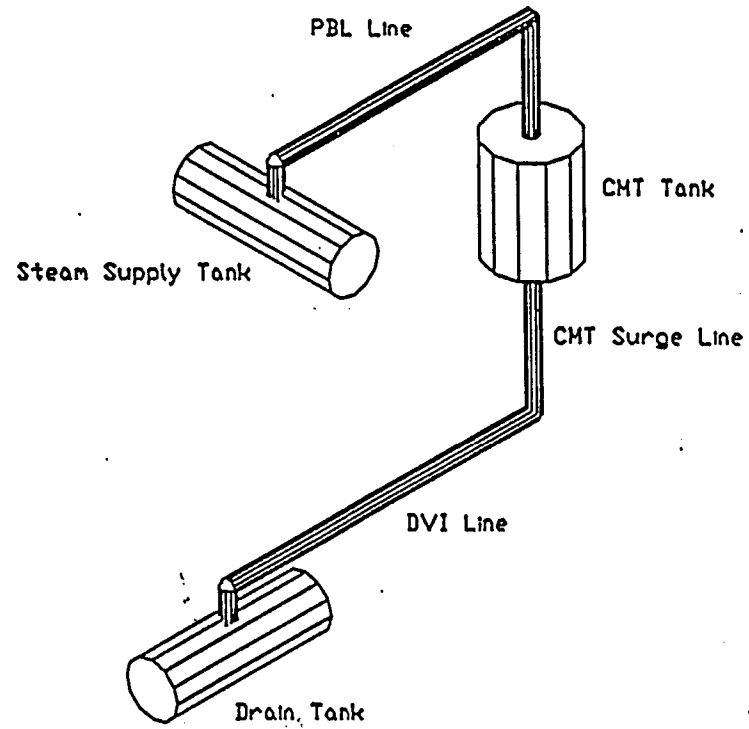


Figure 2.2 Configuration of CMT tank Steam Condensation Test Facility

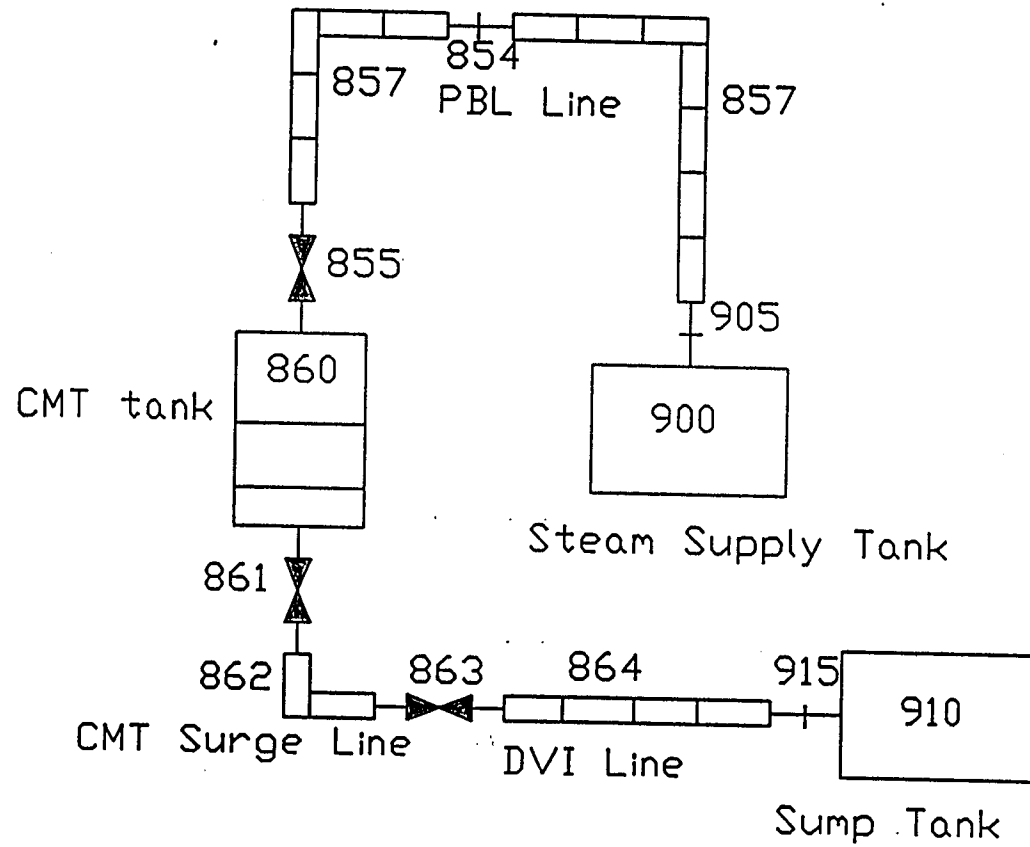


Figure 3.1 Nodalization diagram for base case calculation

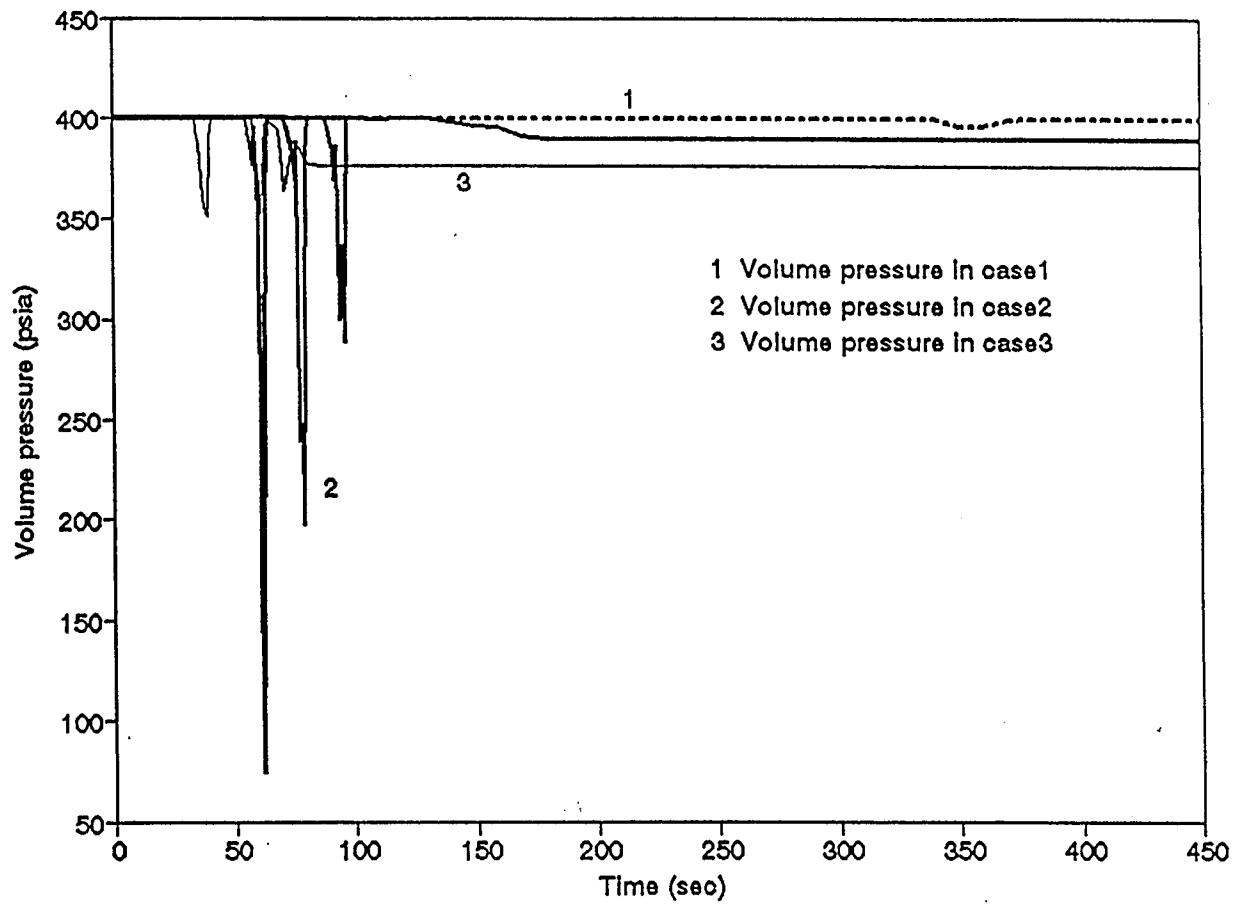


Figure 4.1 Comparison of volume pressure among case 1, 2 and 3

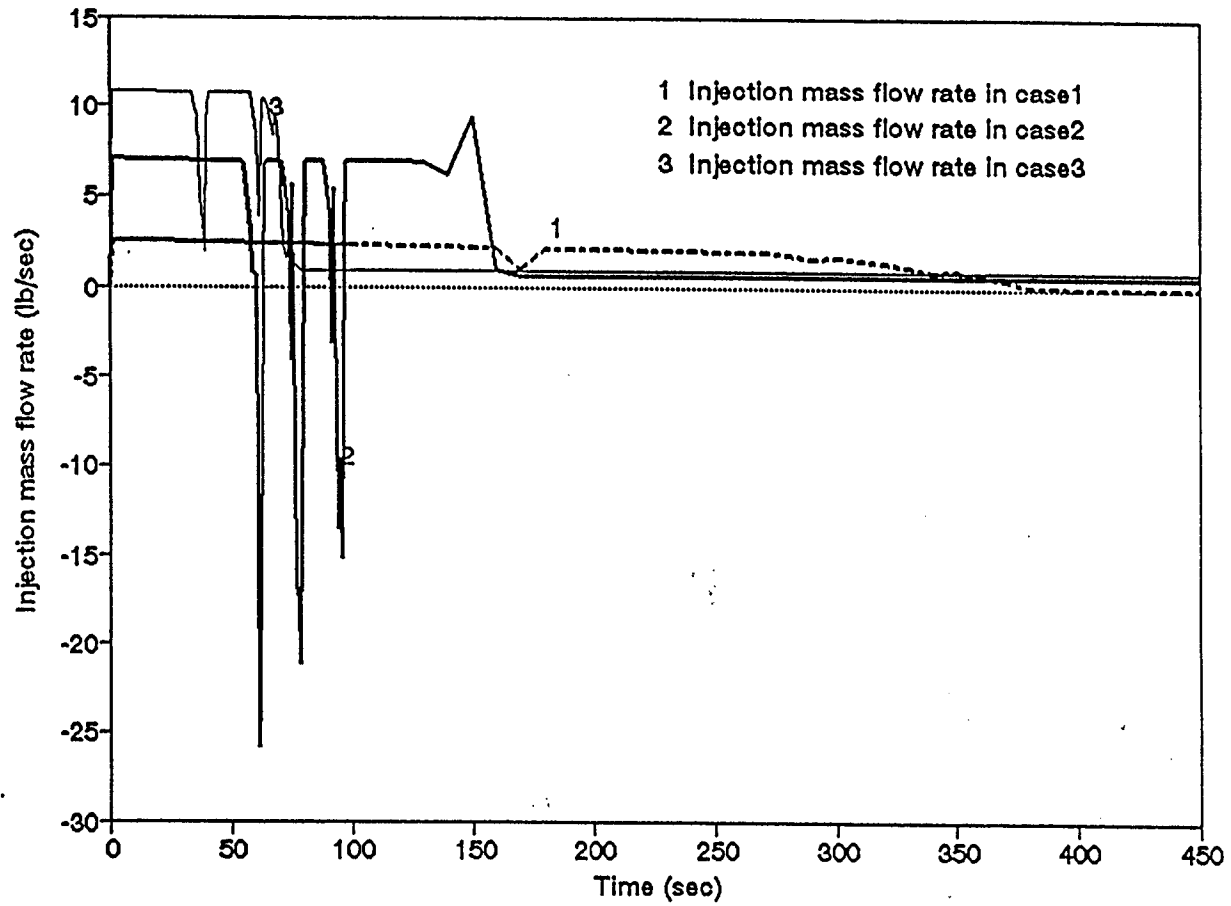


Figure 4.2 Comparison of injection mass flow rate among case 1, 2 and 3

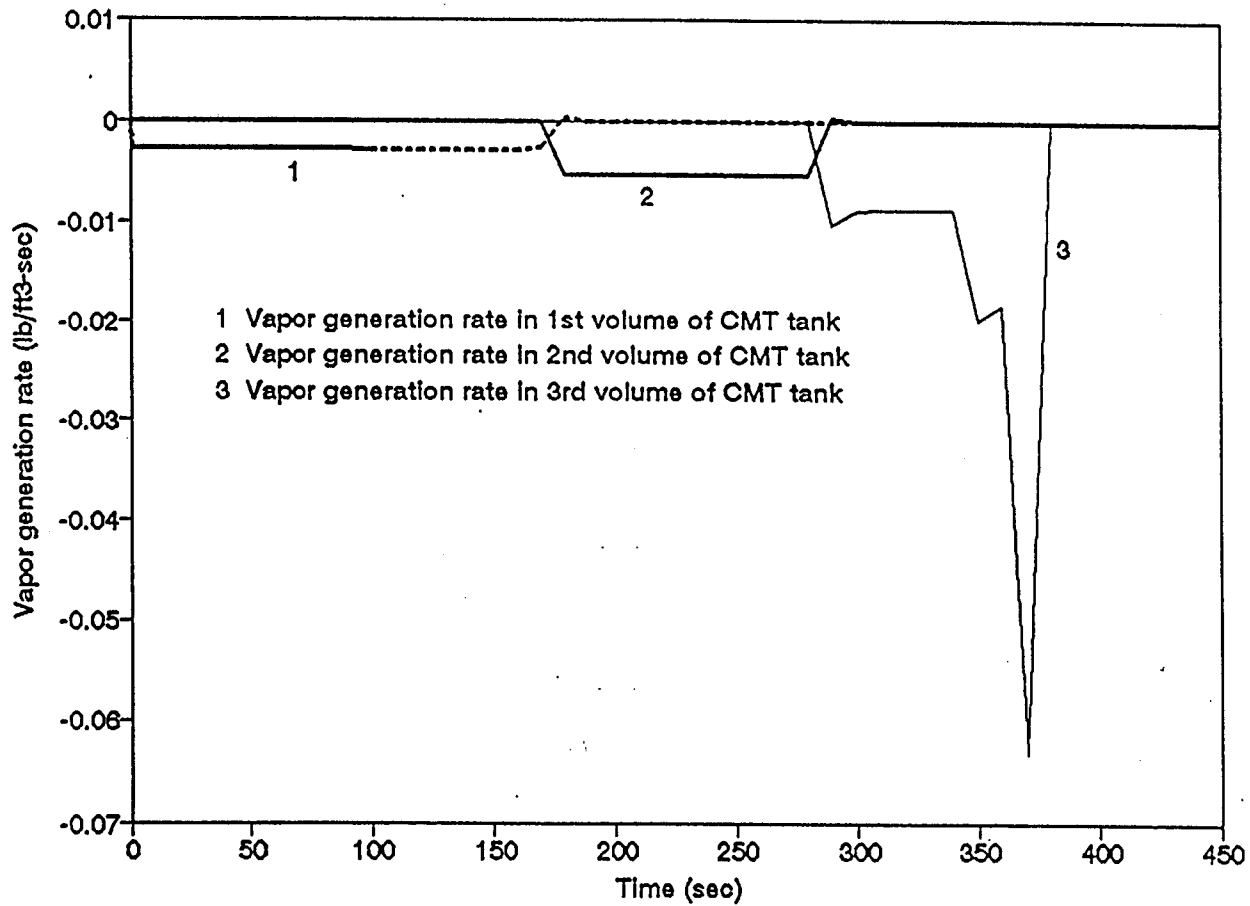


Figure 4.3 CMT tank vapor mass generation rate in case 1

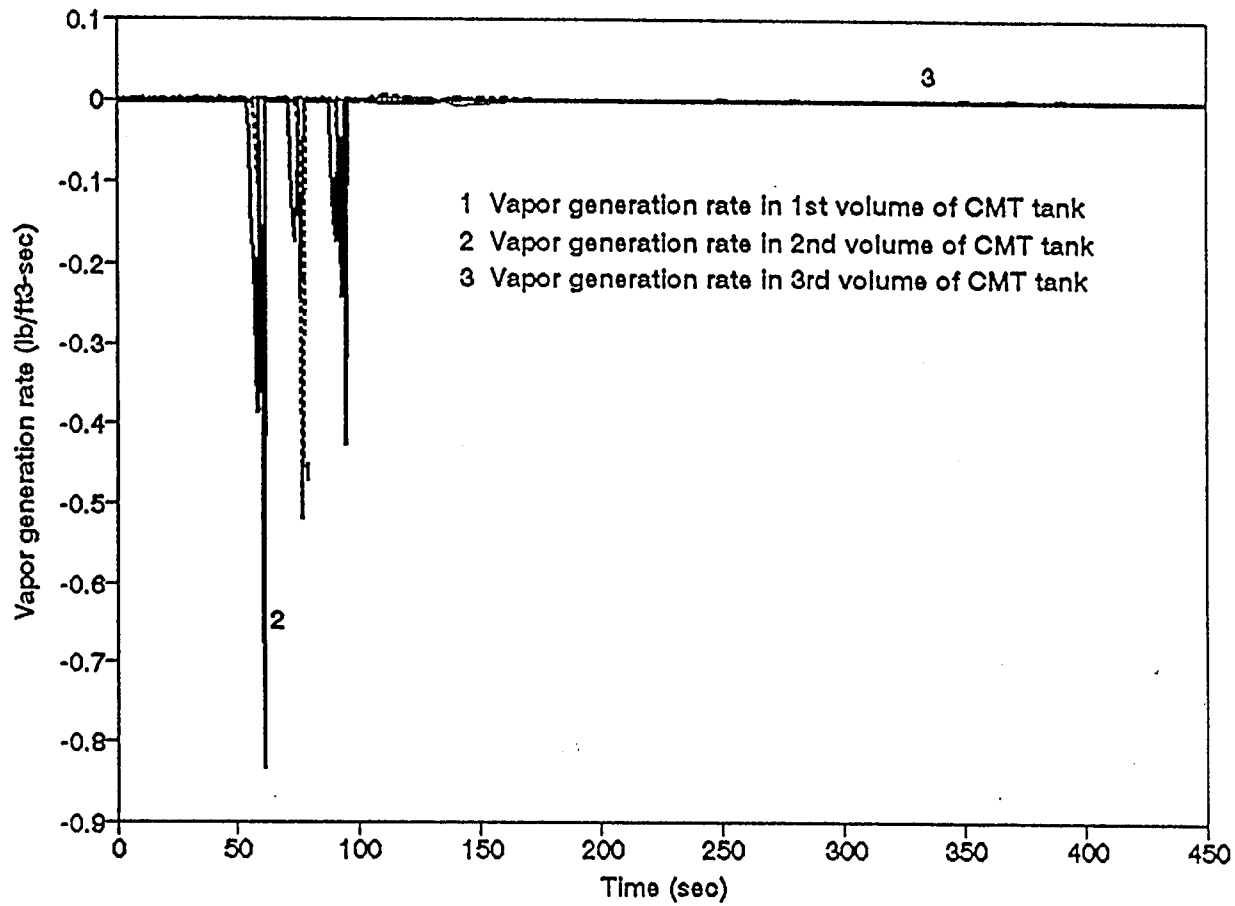


Figure 4.4 CMT tank vapor mass generation rate in case 2

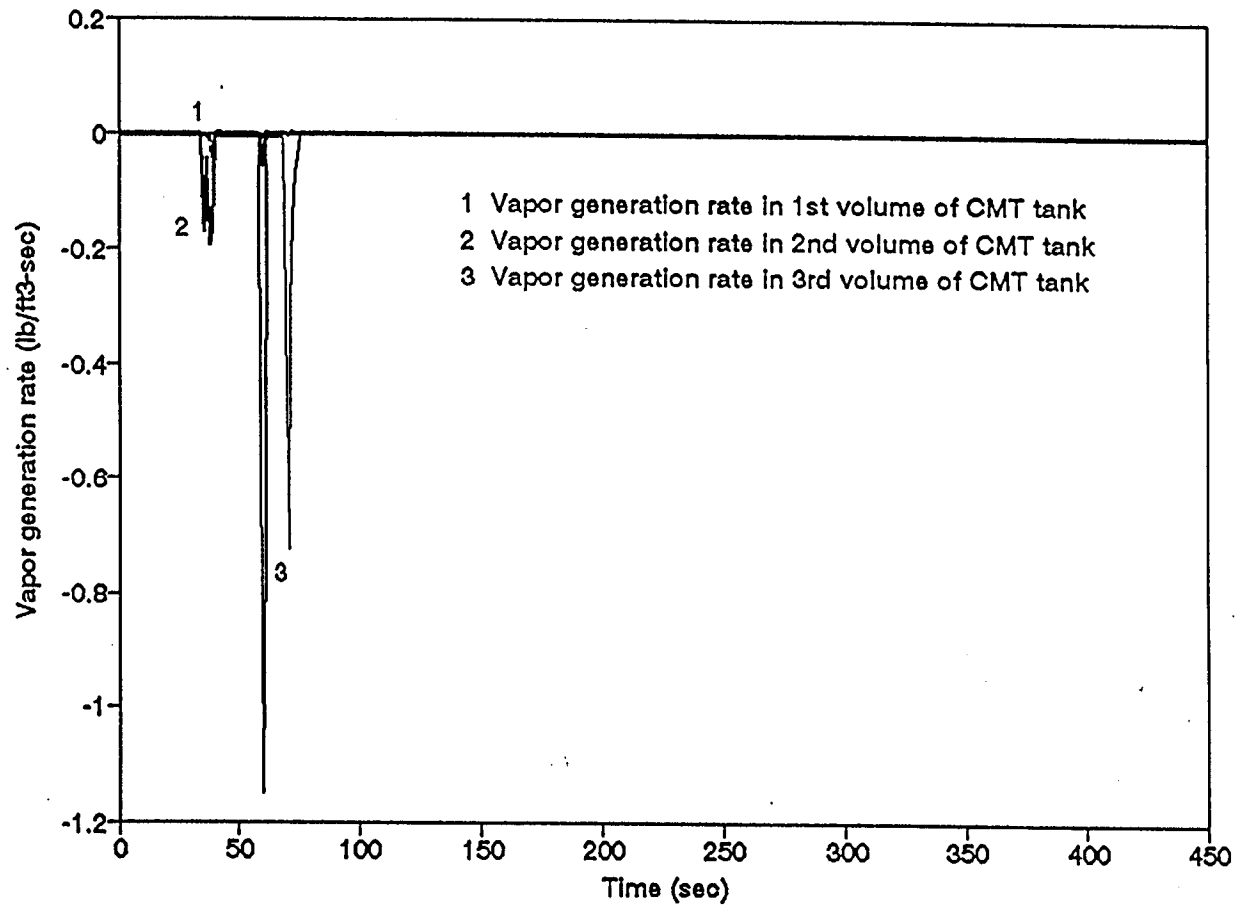


Figure 4.5 CMT tank vapor mass generation rate in case 3

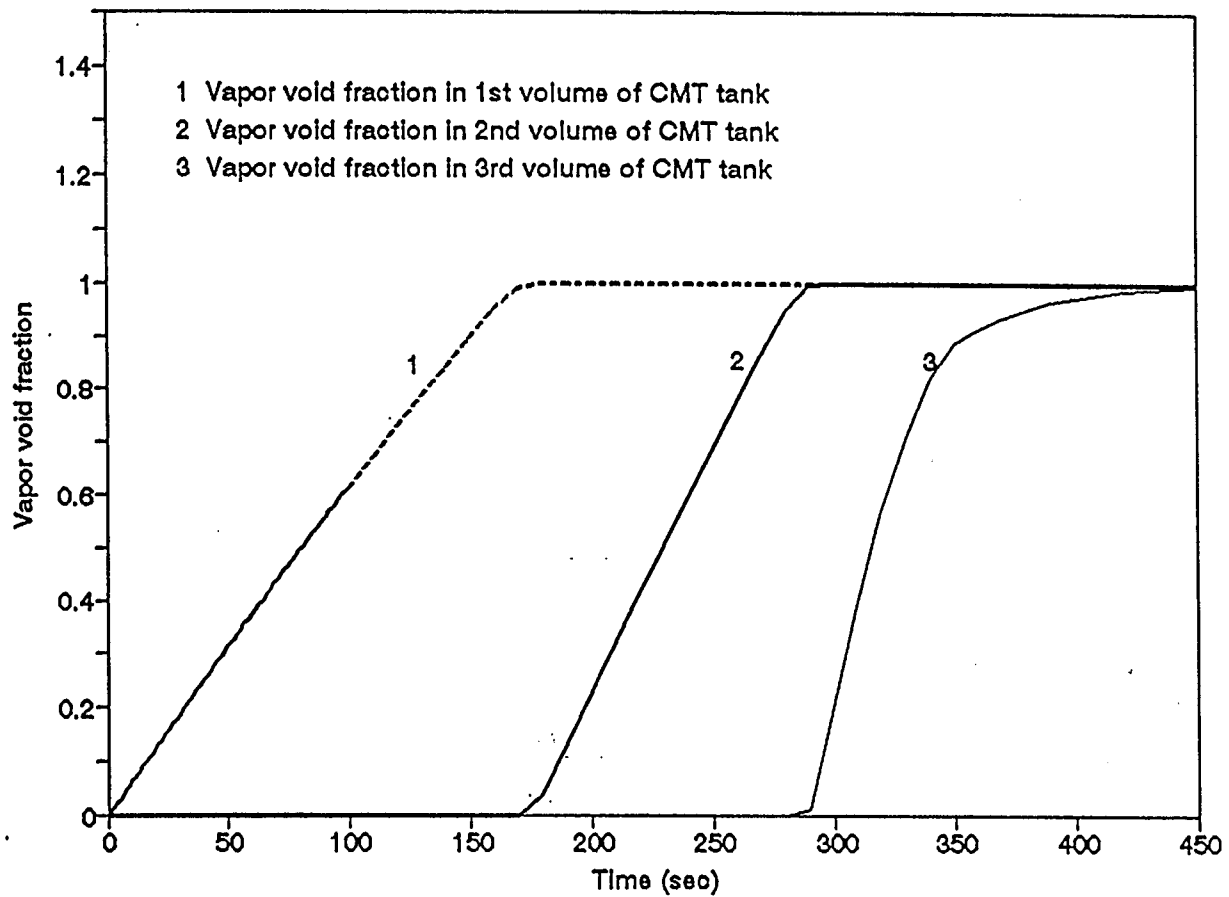


Figure 4.6 CMT tank vapor void fraction changed with time in case 1

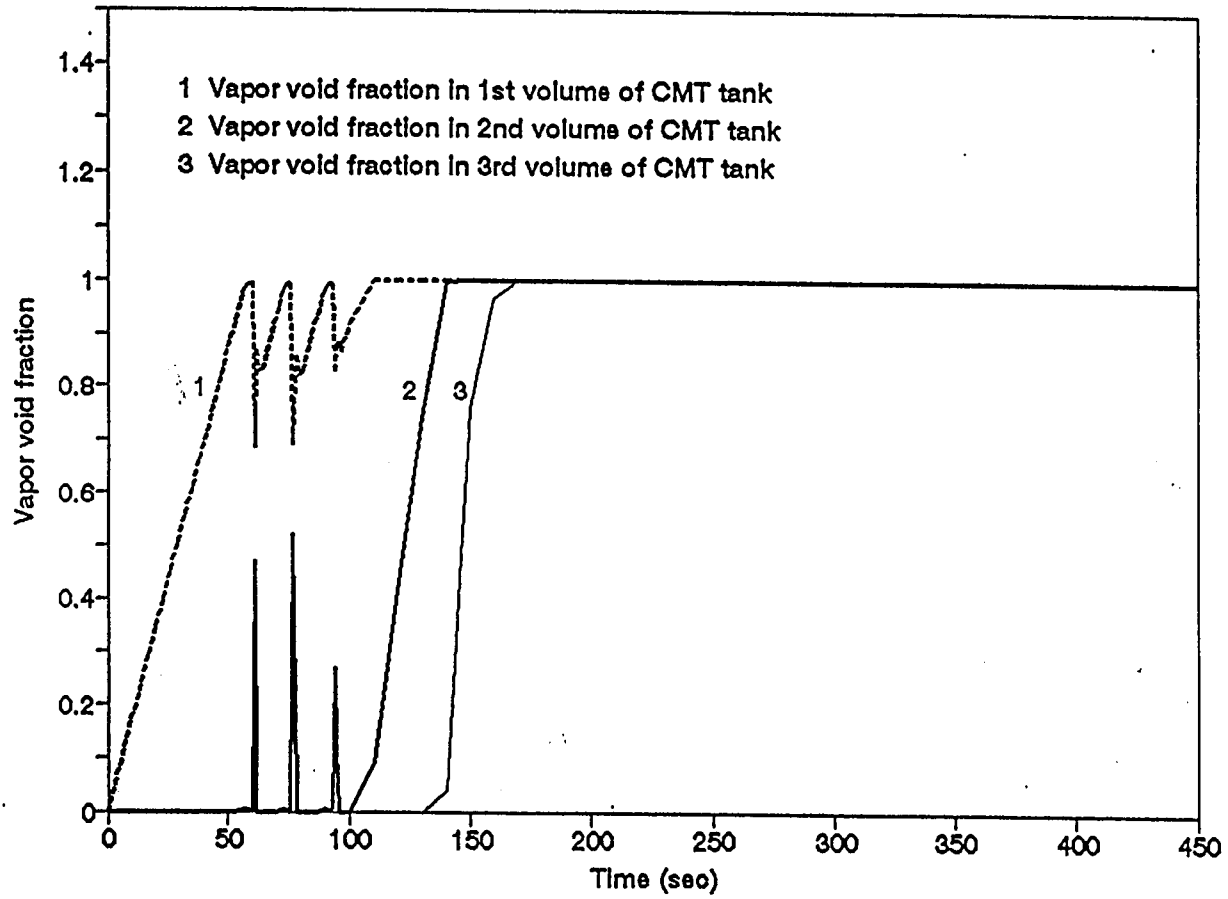


Figure 4.7 CMT tank vapor void fraction changed with time in case 2

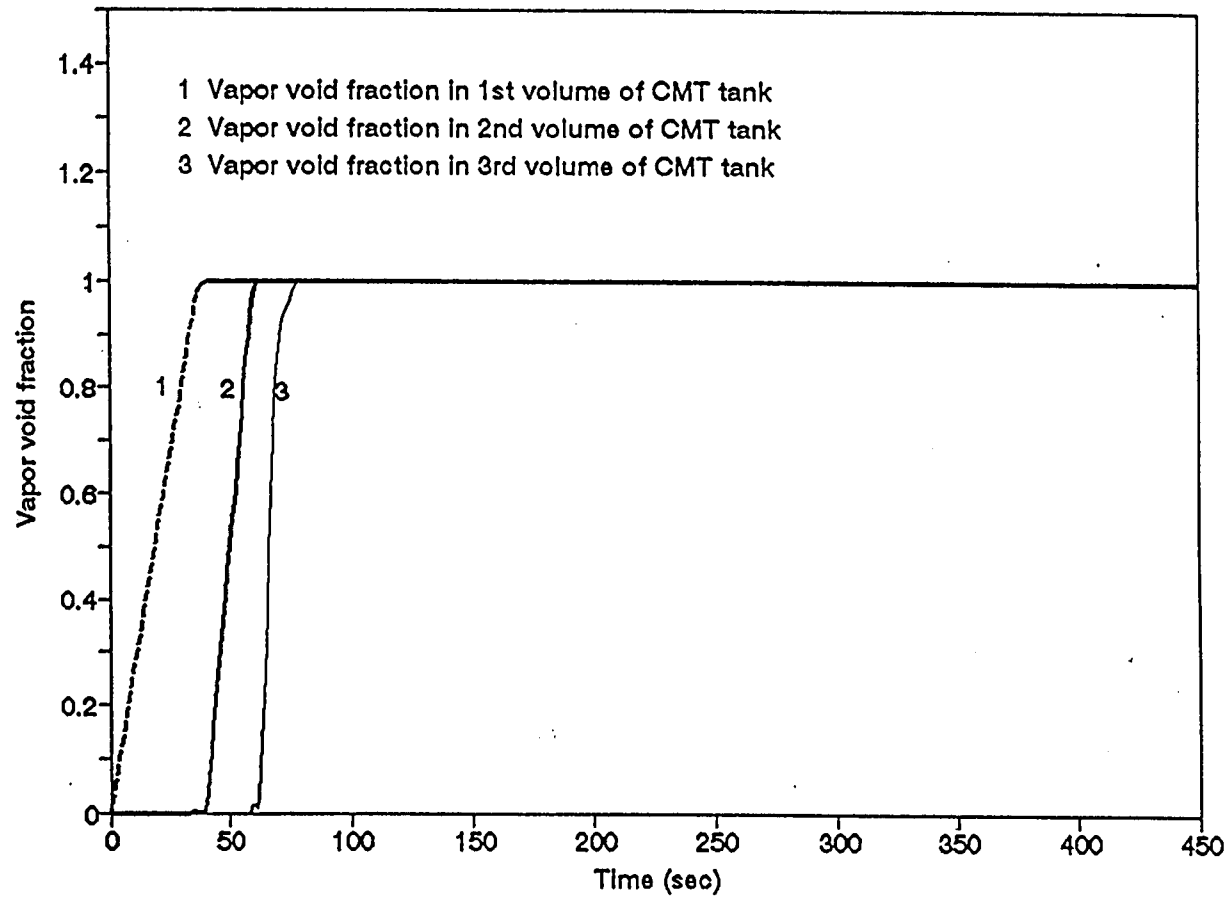


Figure 4.8 CMT tank vapor void fraction changed with time in case 3

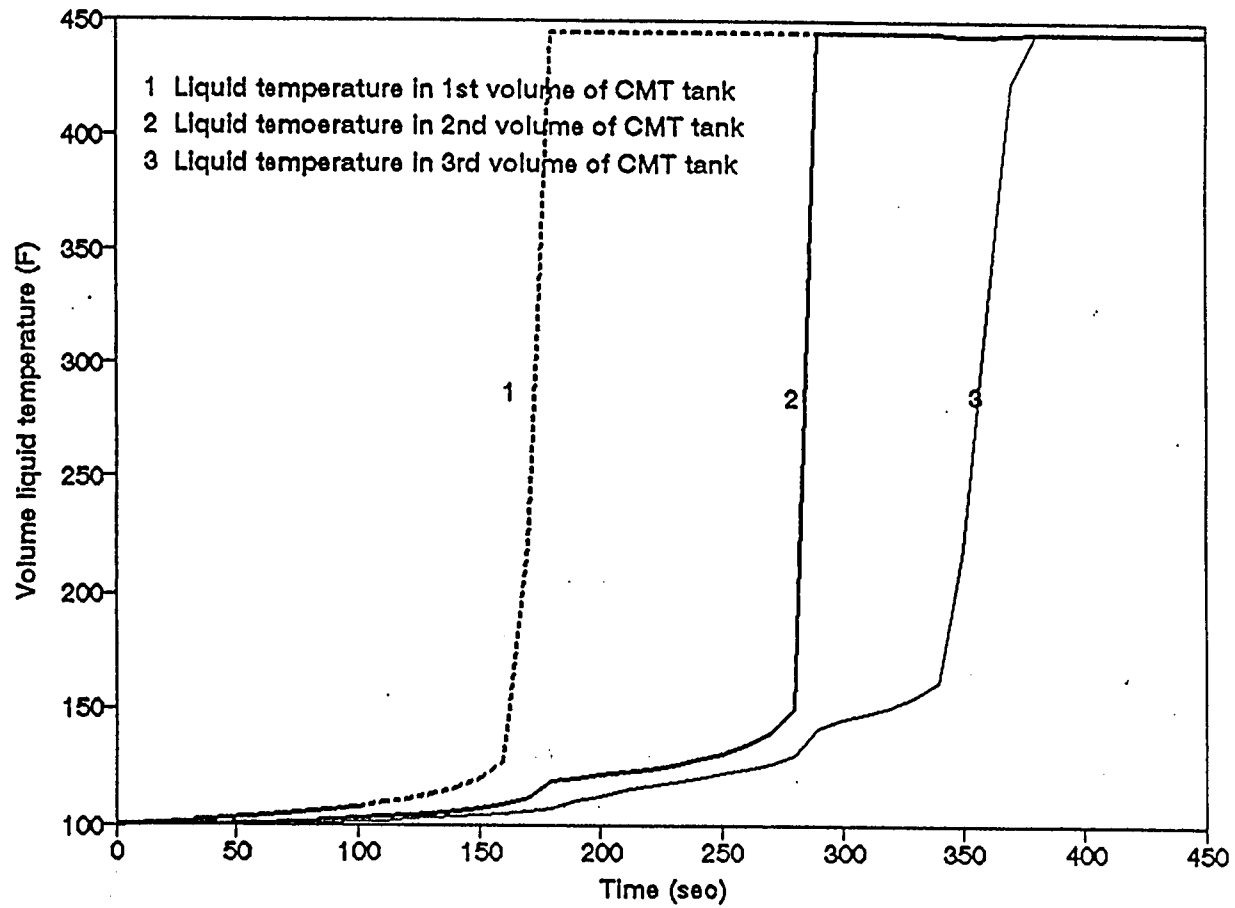


Figure 4.9 CMT tank liquid temperature changed with time in case 1

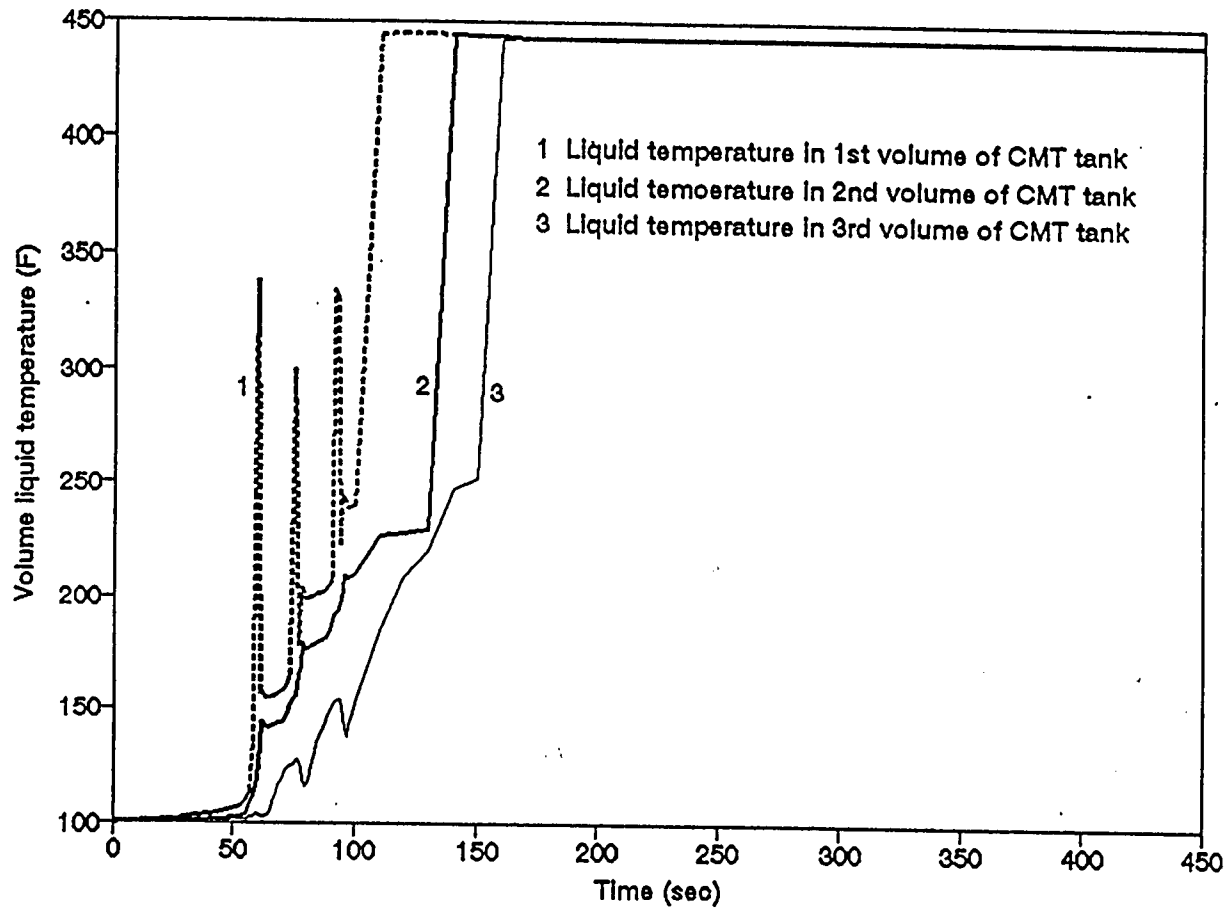


Figure 4.10 CMT tank liquid temperature changed with time in case 2

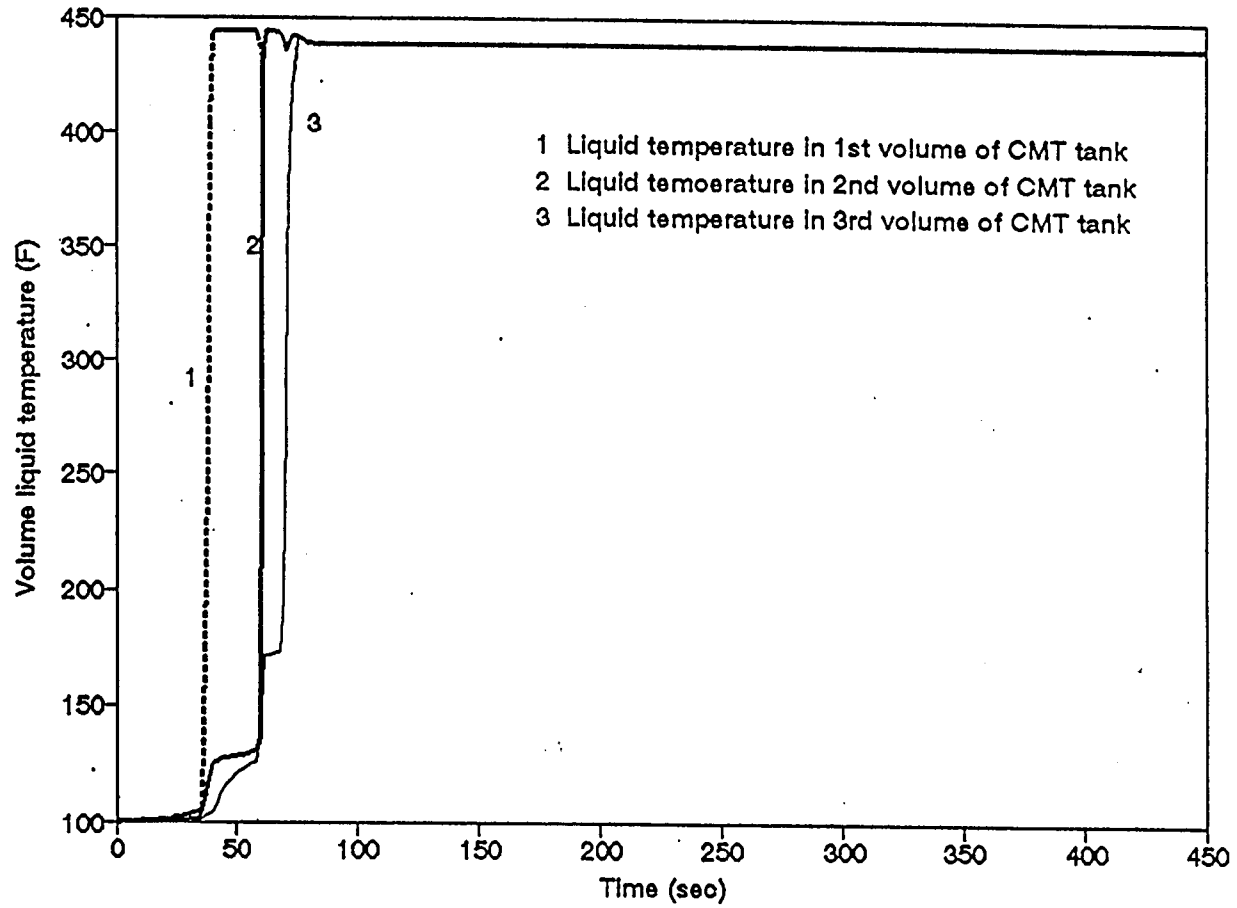


Figure 4.11 CMT tank liquid temperature changed with time in case 3

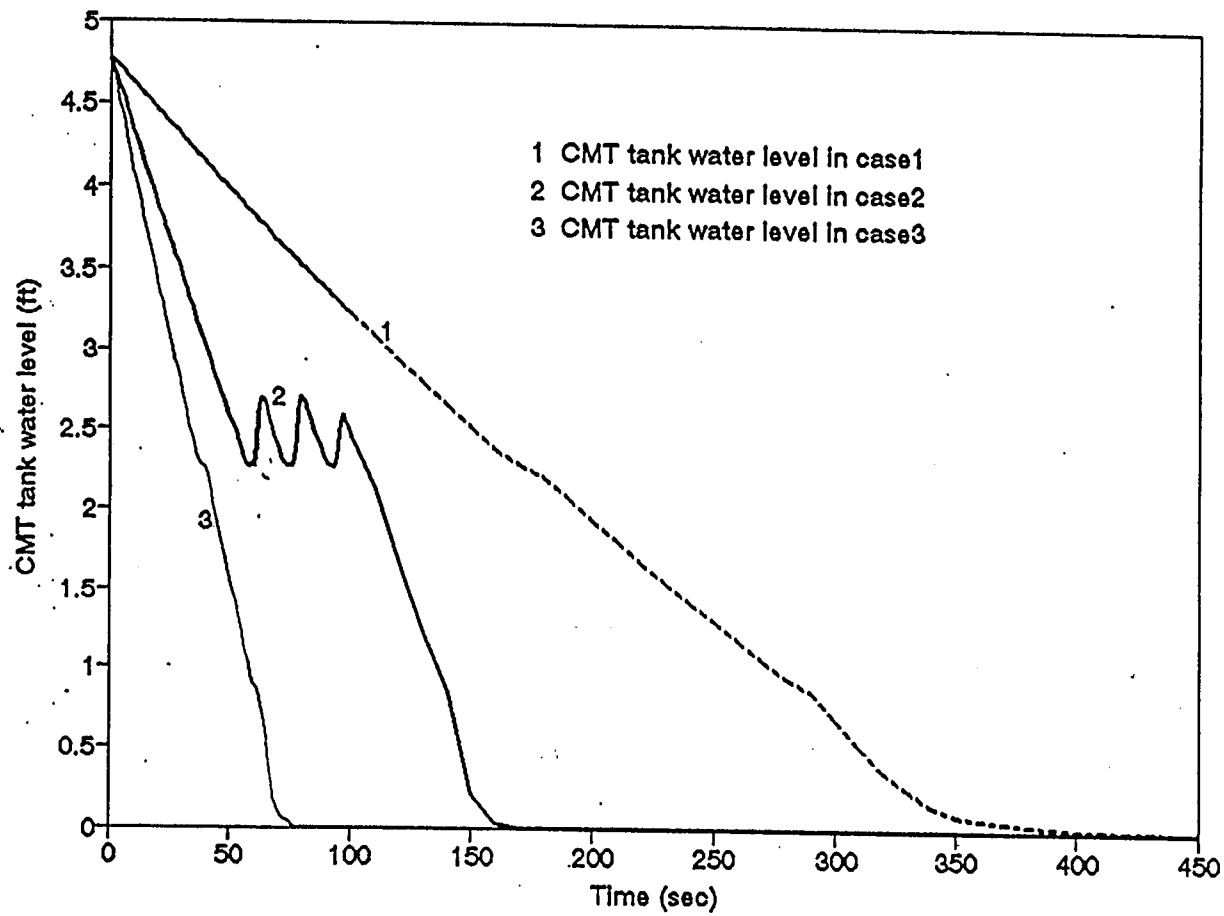


Figure 4.12 Comparison of CMT tank water level in case 1, 2, and 3

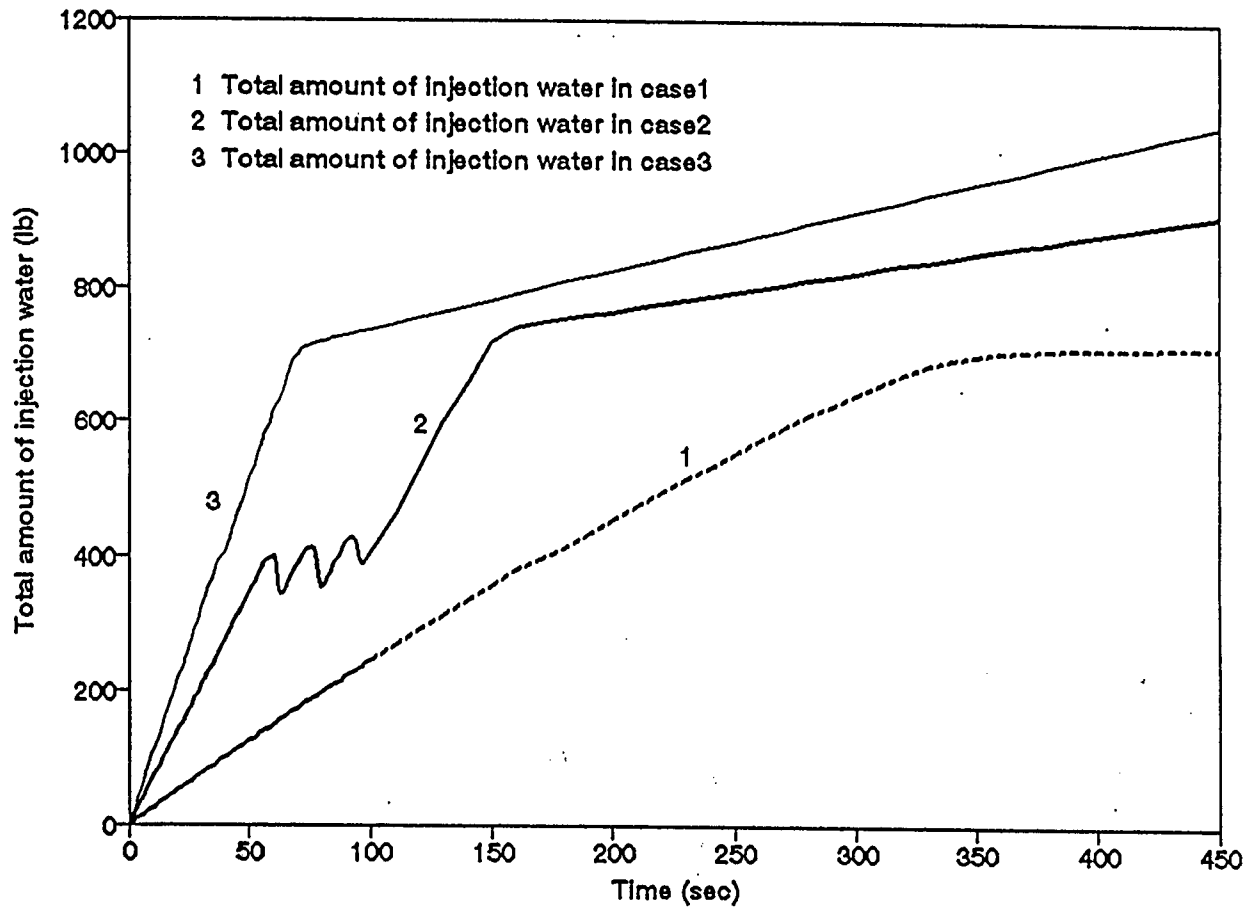


Figure 4.13 Comparison of CMT tank total amount of injection water in case 1, case 2, and case 3

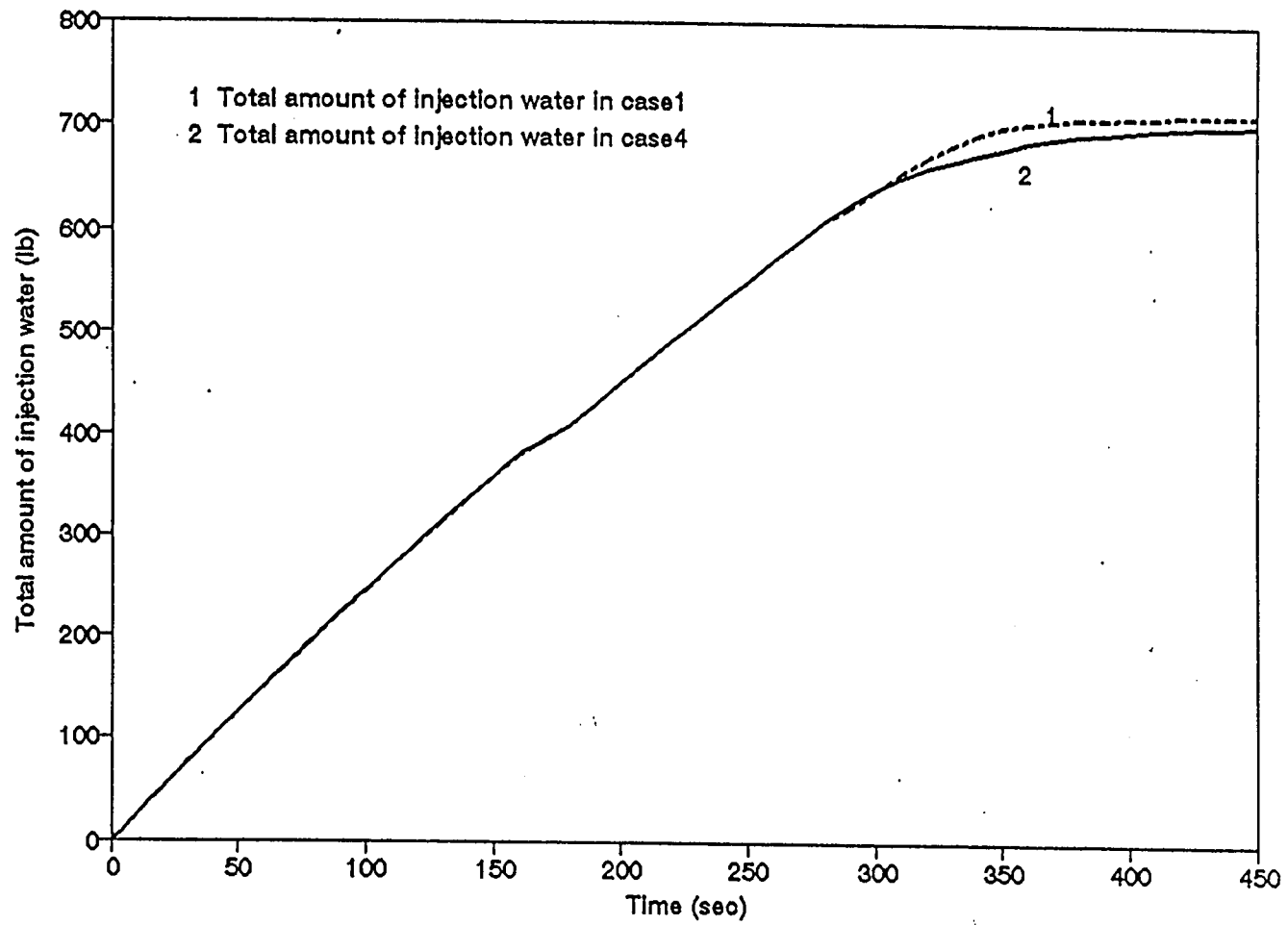


Figure 4.14 Comparison of CMT tank total amount of injection water between case 1 and case 4

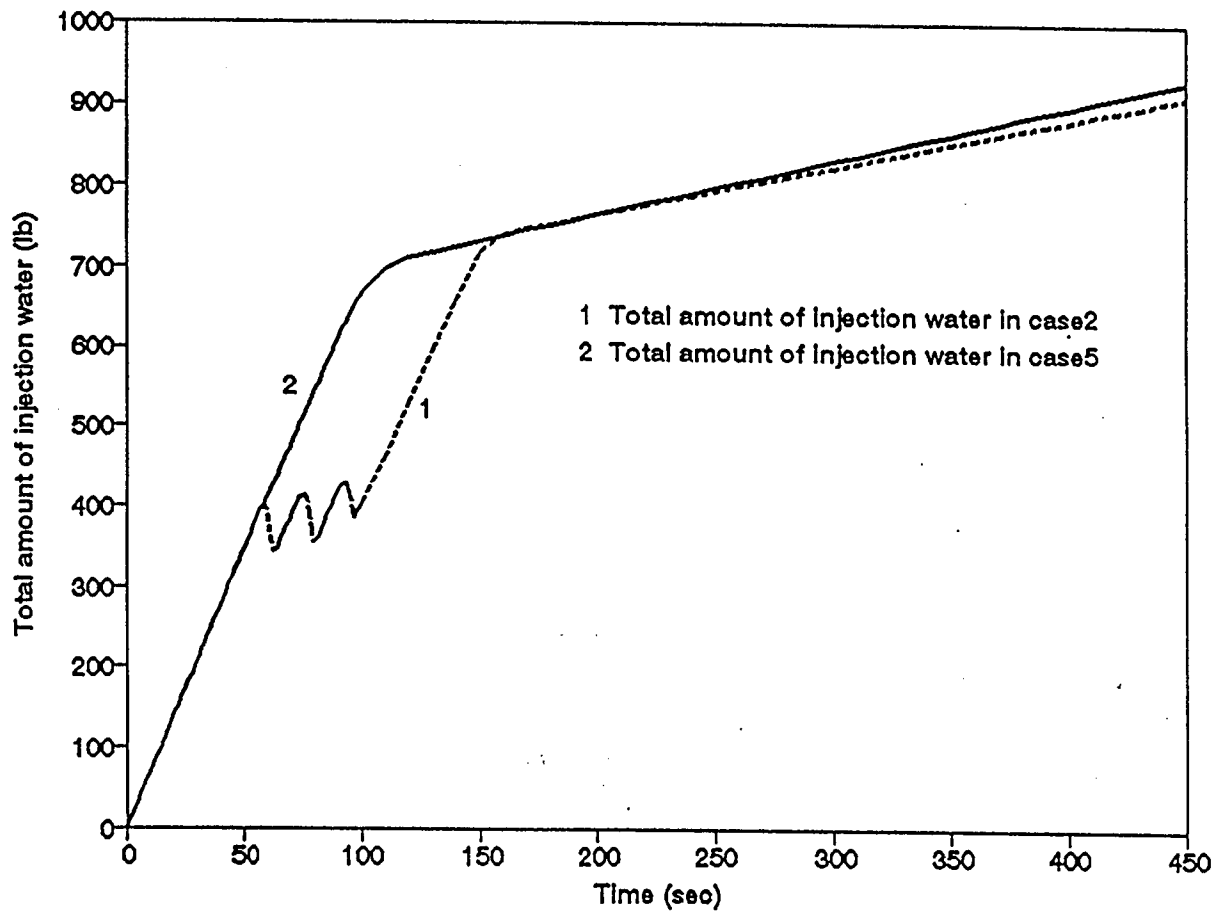


Figure 4.15 Comparison of CMT tank total amount of injection water between case 2 and case 5

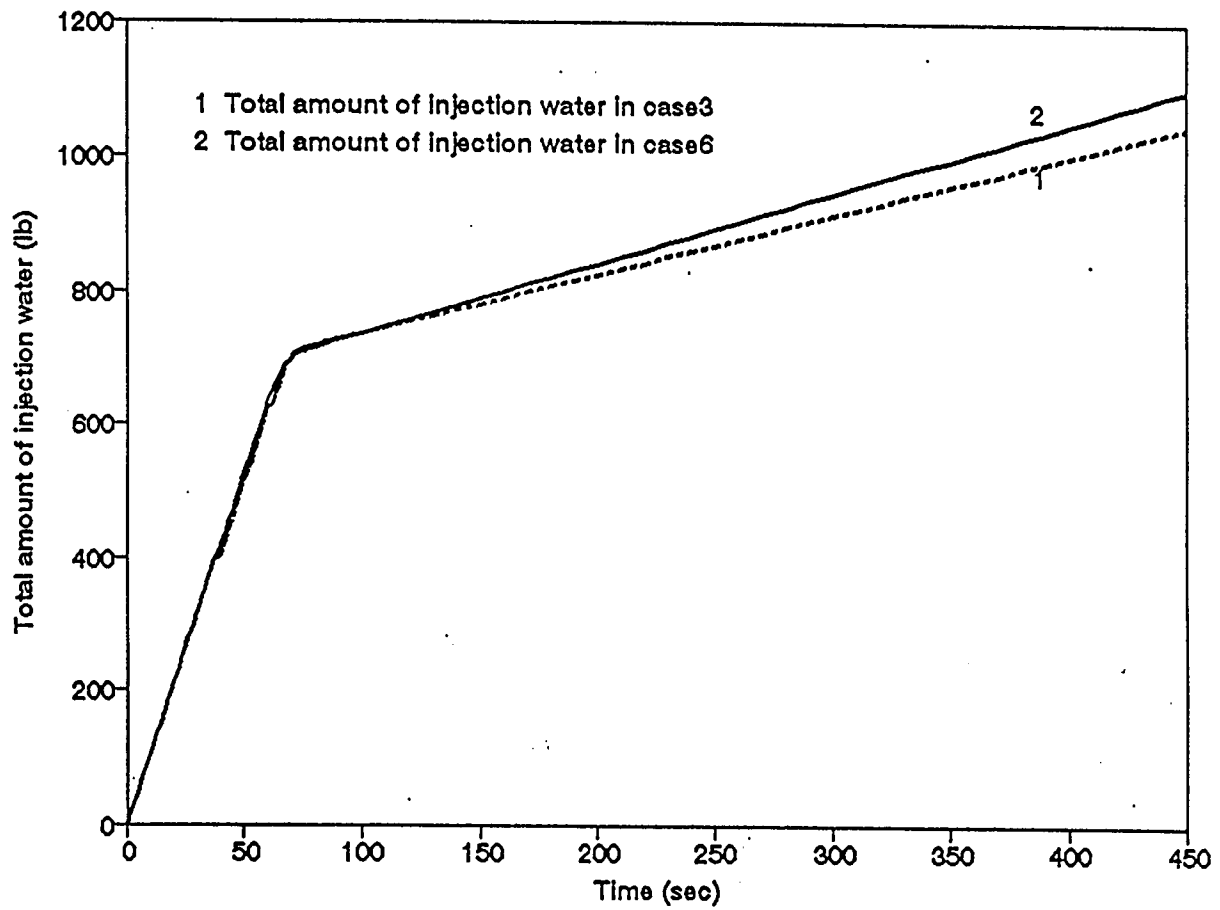


Figure 4.16 Comparison of CMT tank total amount of injection water between case 3 and case 6

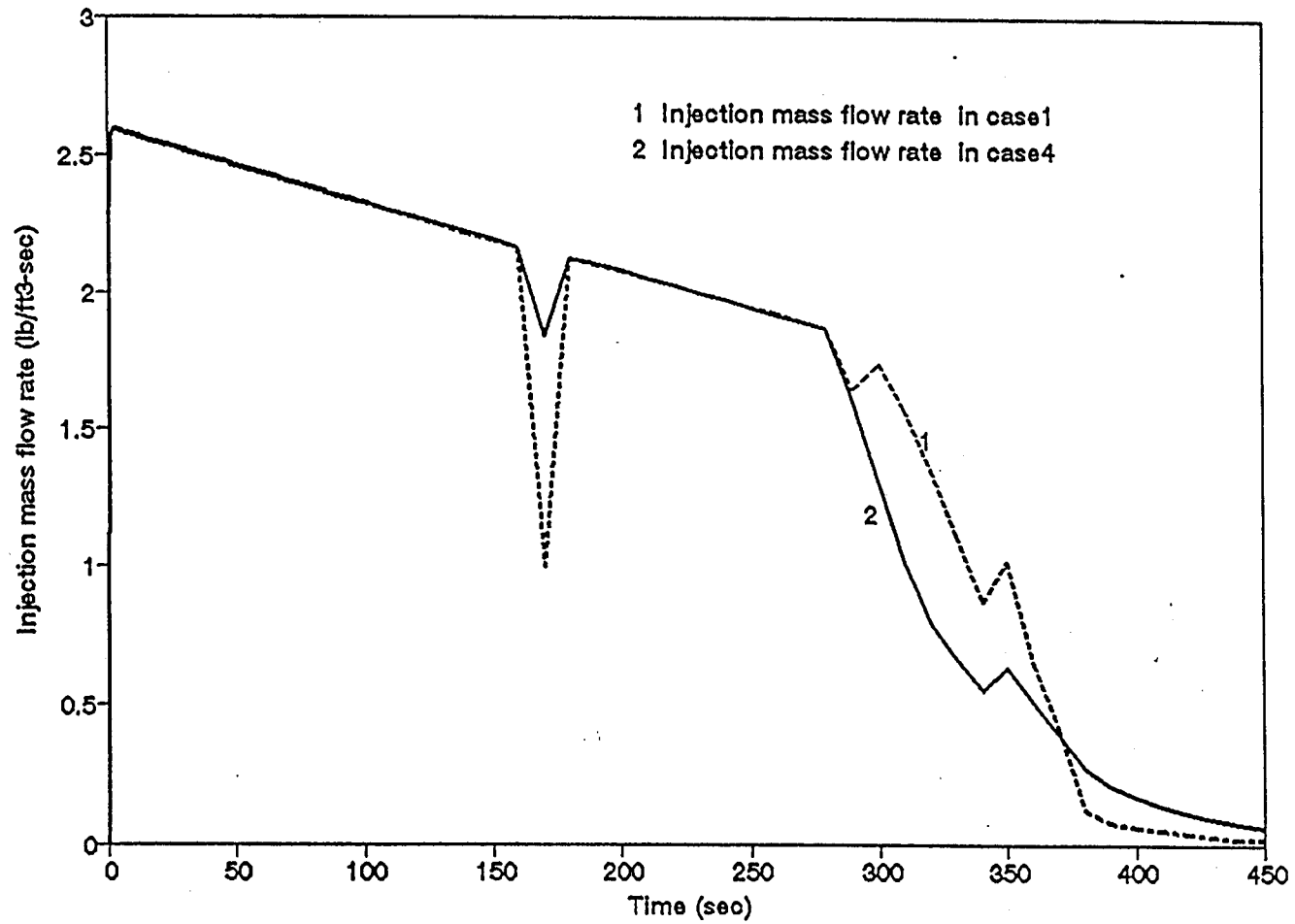


Figure 4.17 Comparison of CMT tank injection mass flow rate between case 1 and case 4

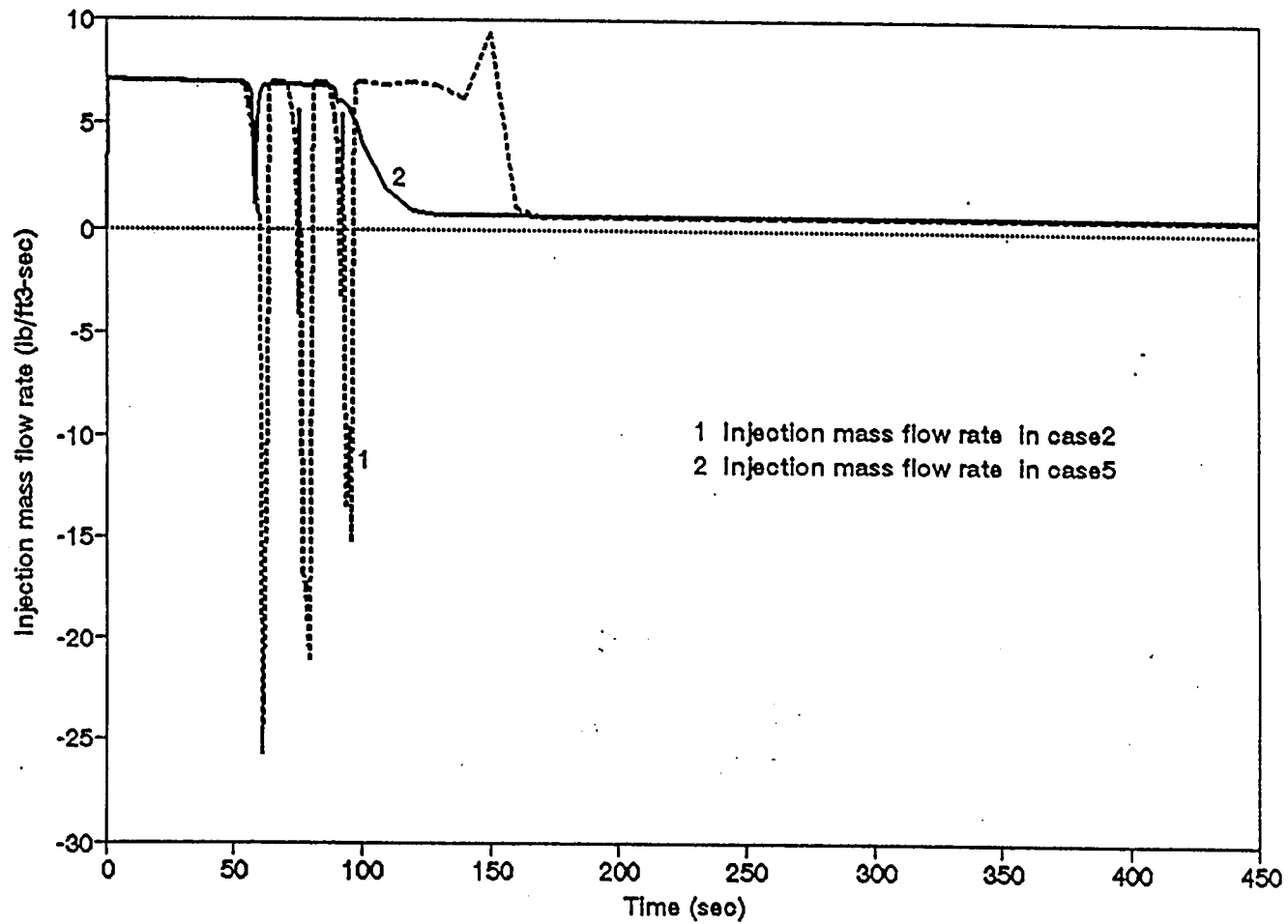


Figure 4.18 Comparison of CMT tank injection mass flow rate between case 2 and case 5

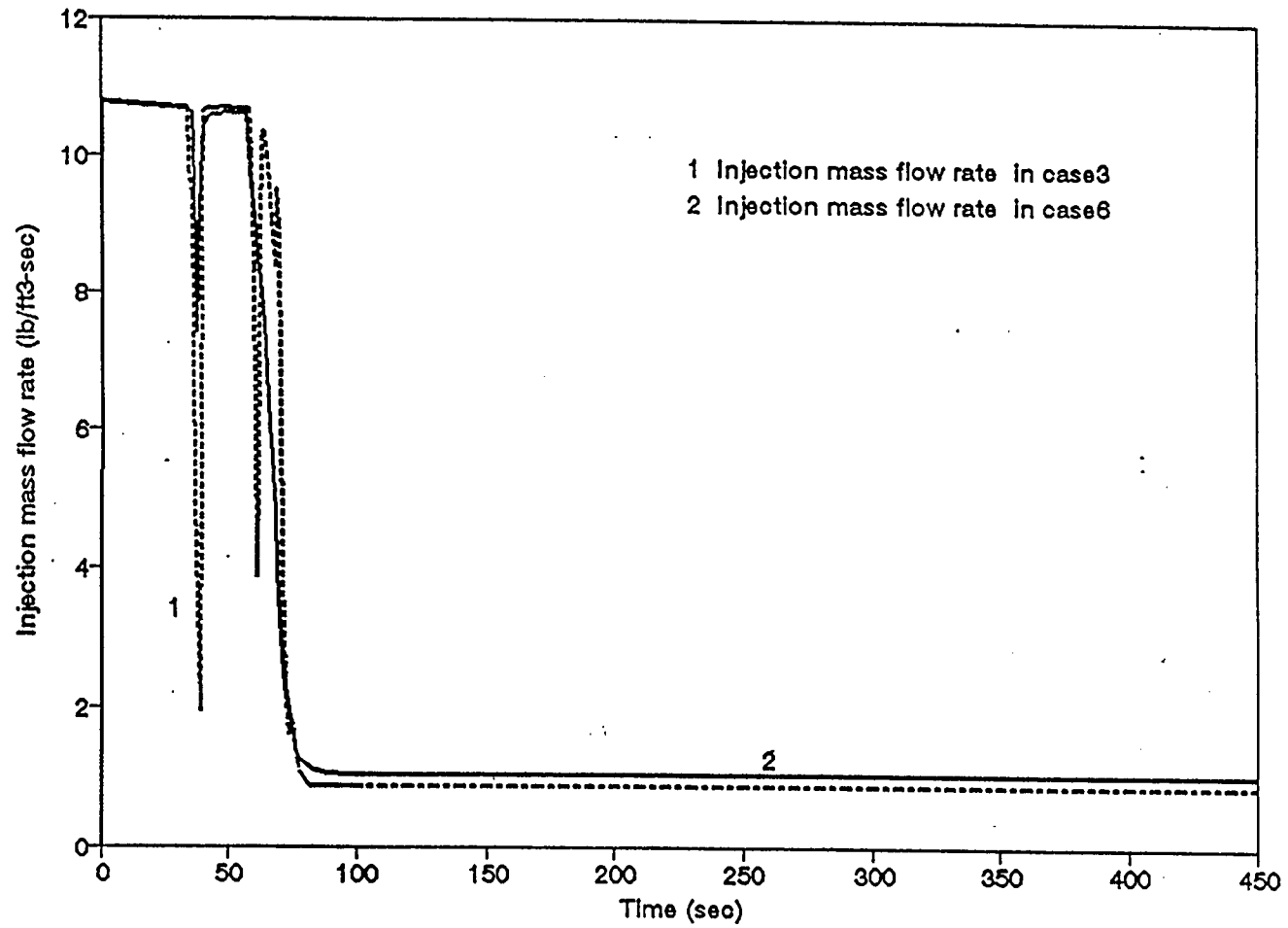


Figure 4.19 Comparison of CMT tank injection mass flow rate between case 3 and case 6

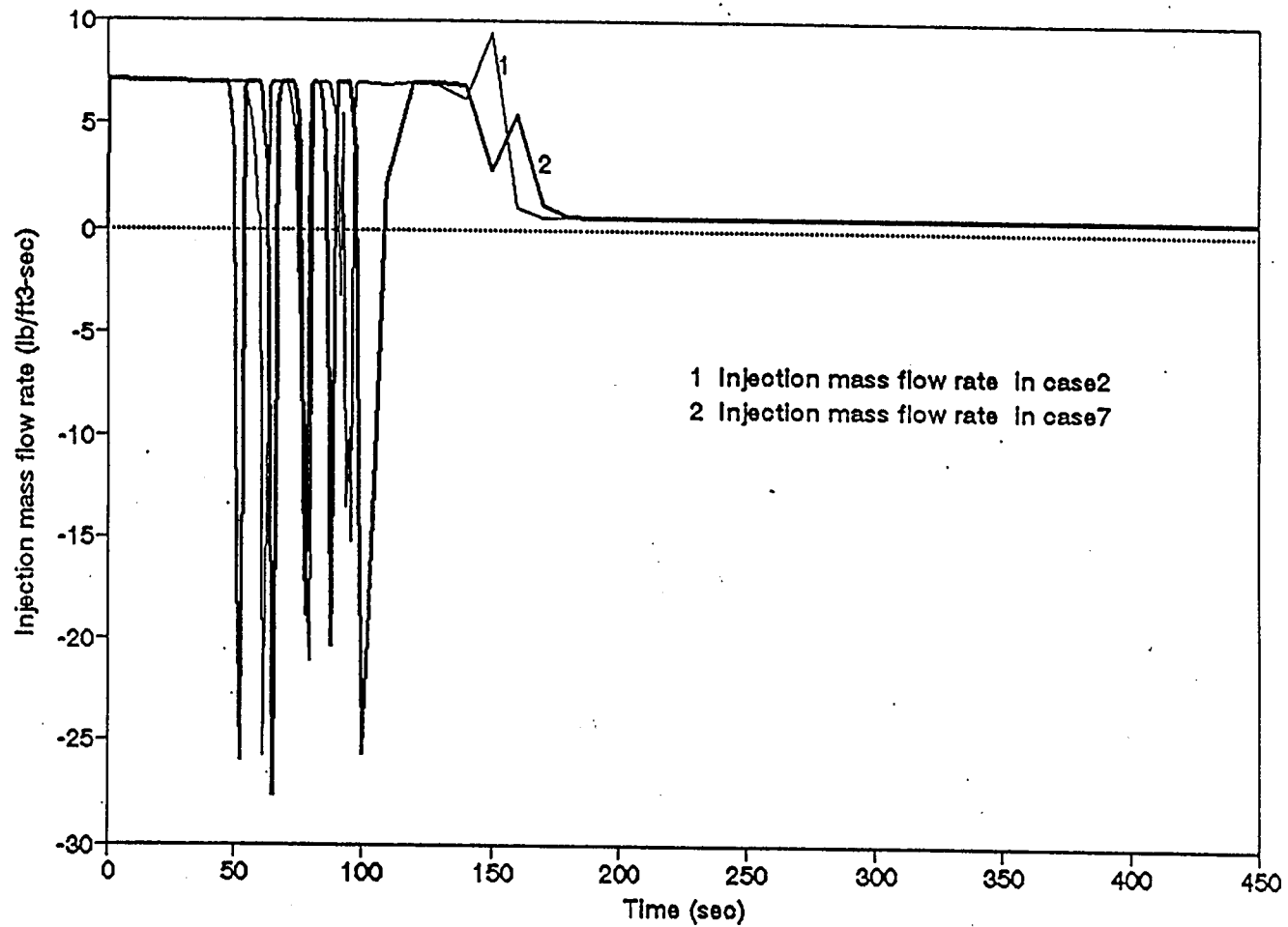


Figure 4.20 Comparison of CMT tank injection mass flow rate between case 2 and case 7

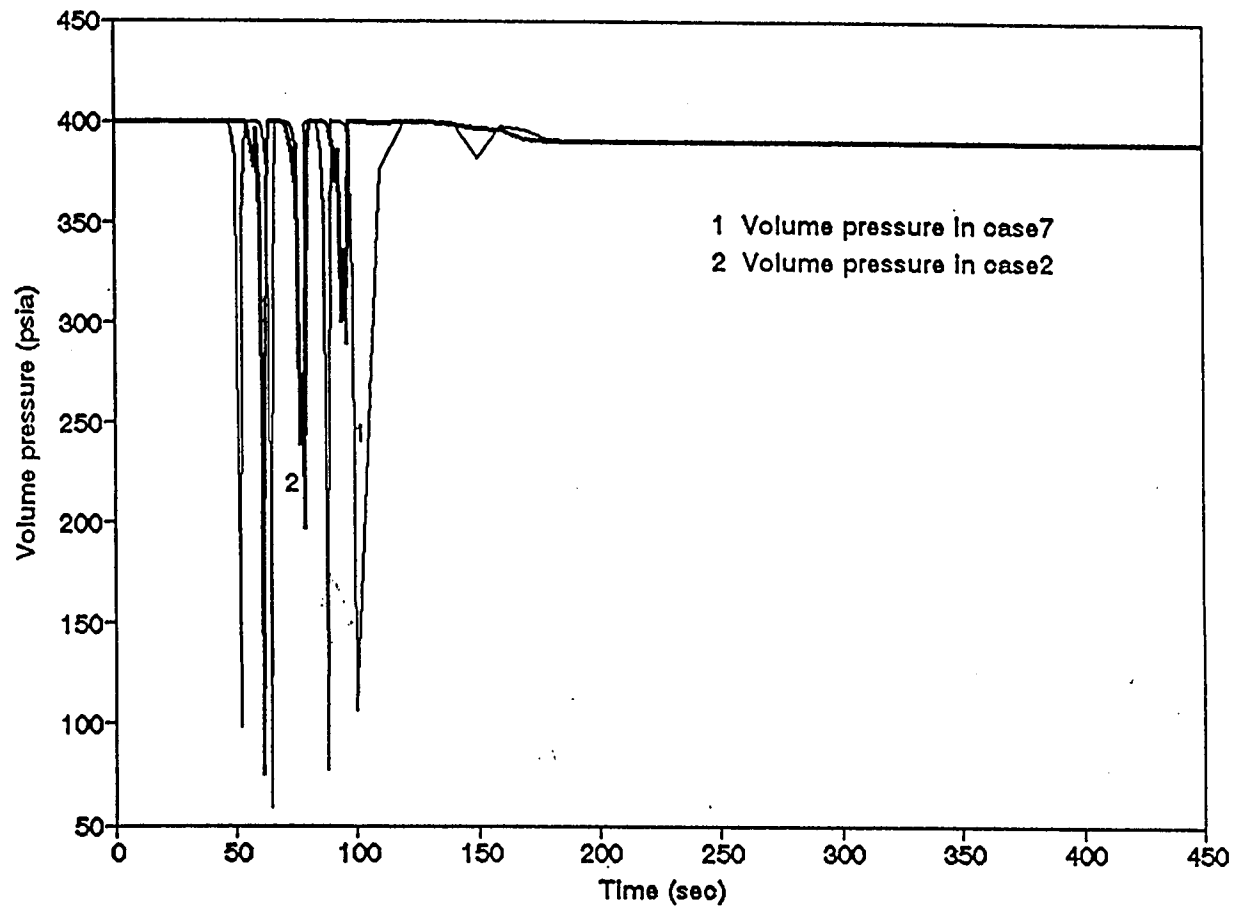


Figure 4.21 Comparison of pressure in CMT tank between case 2 and case 7

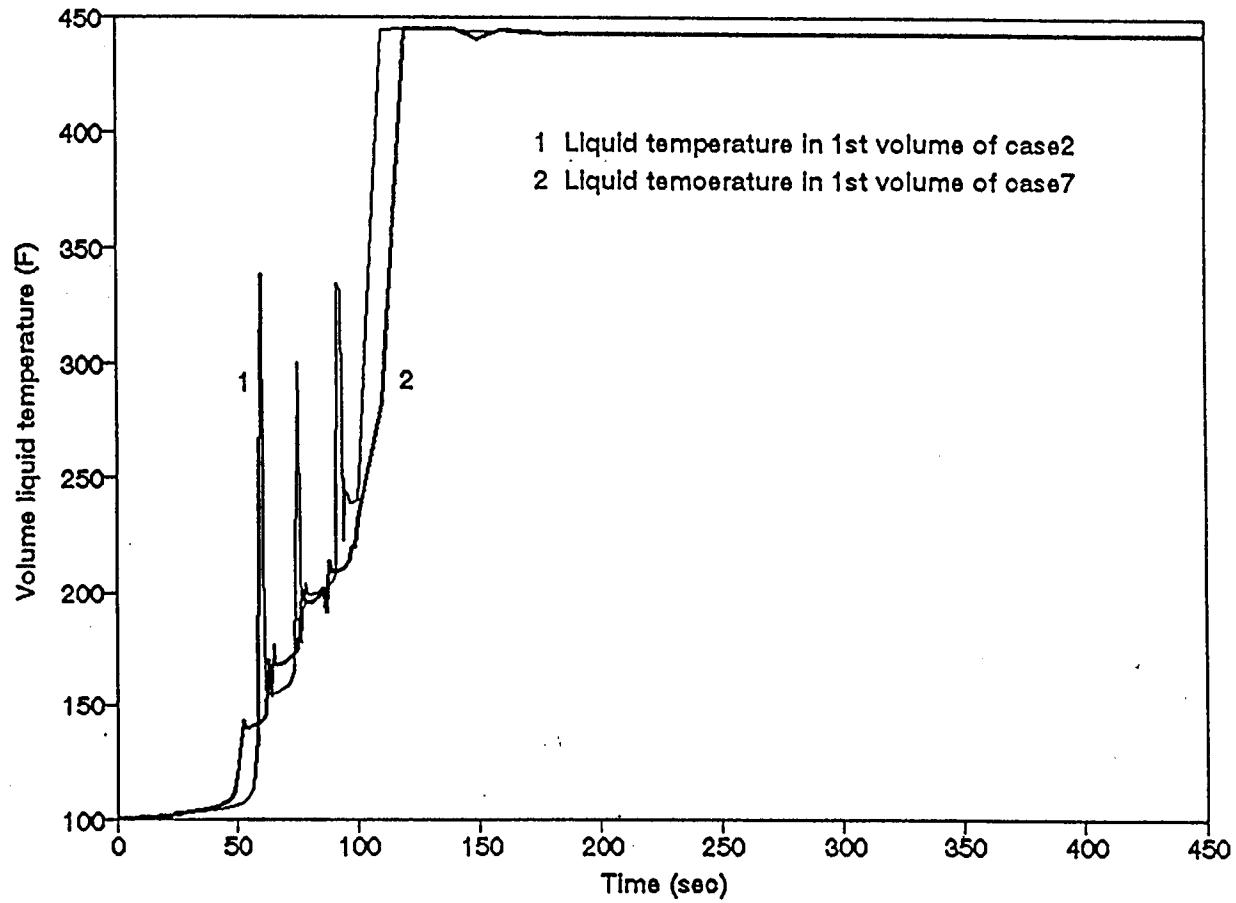


Figure 4.22 Comparison of temperature of 1st volume in CMT tank between case 2 and case 7

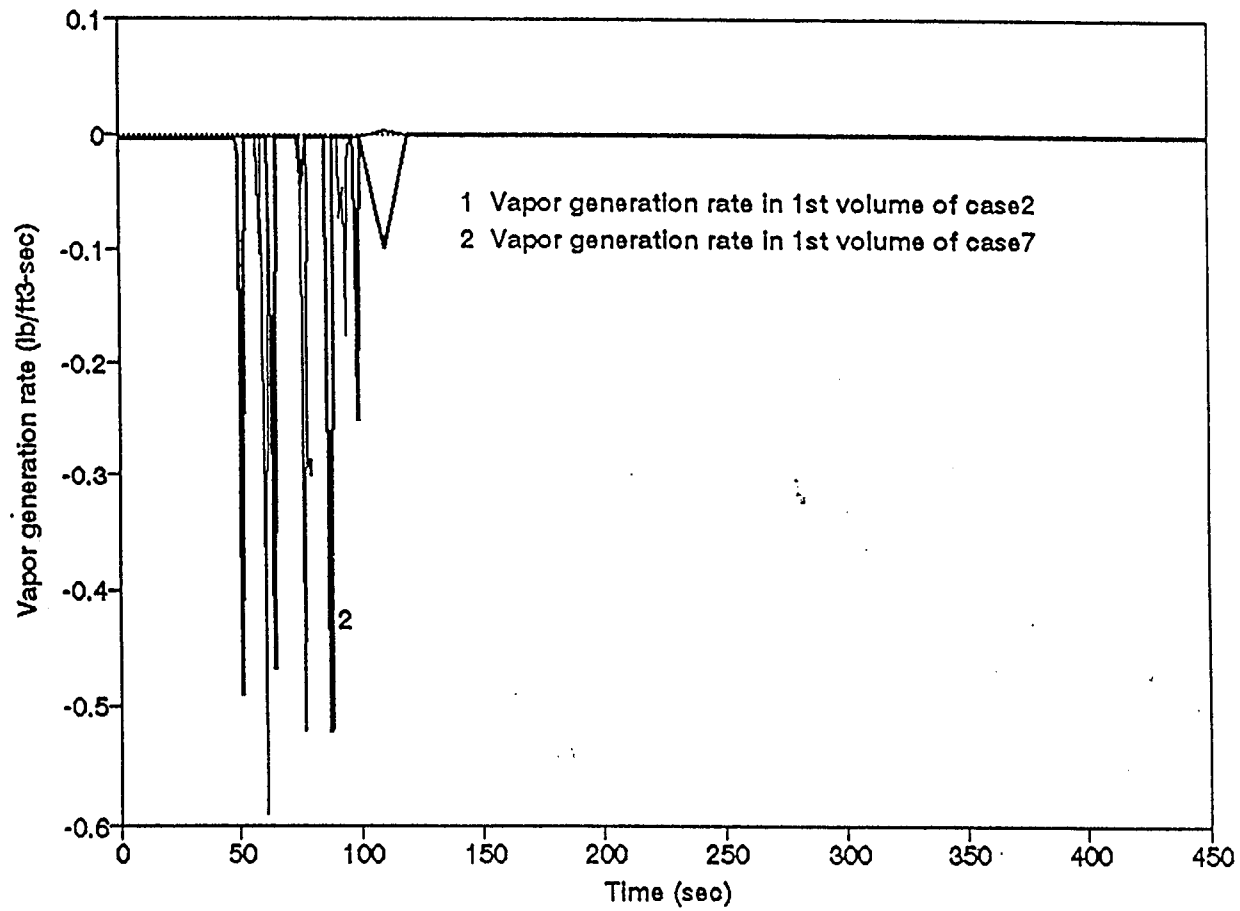


Figure 4.23 Comparison of 1st volume vapor mass generation rate in CMT tank between case 2 and case 7

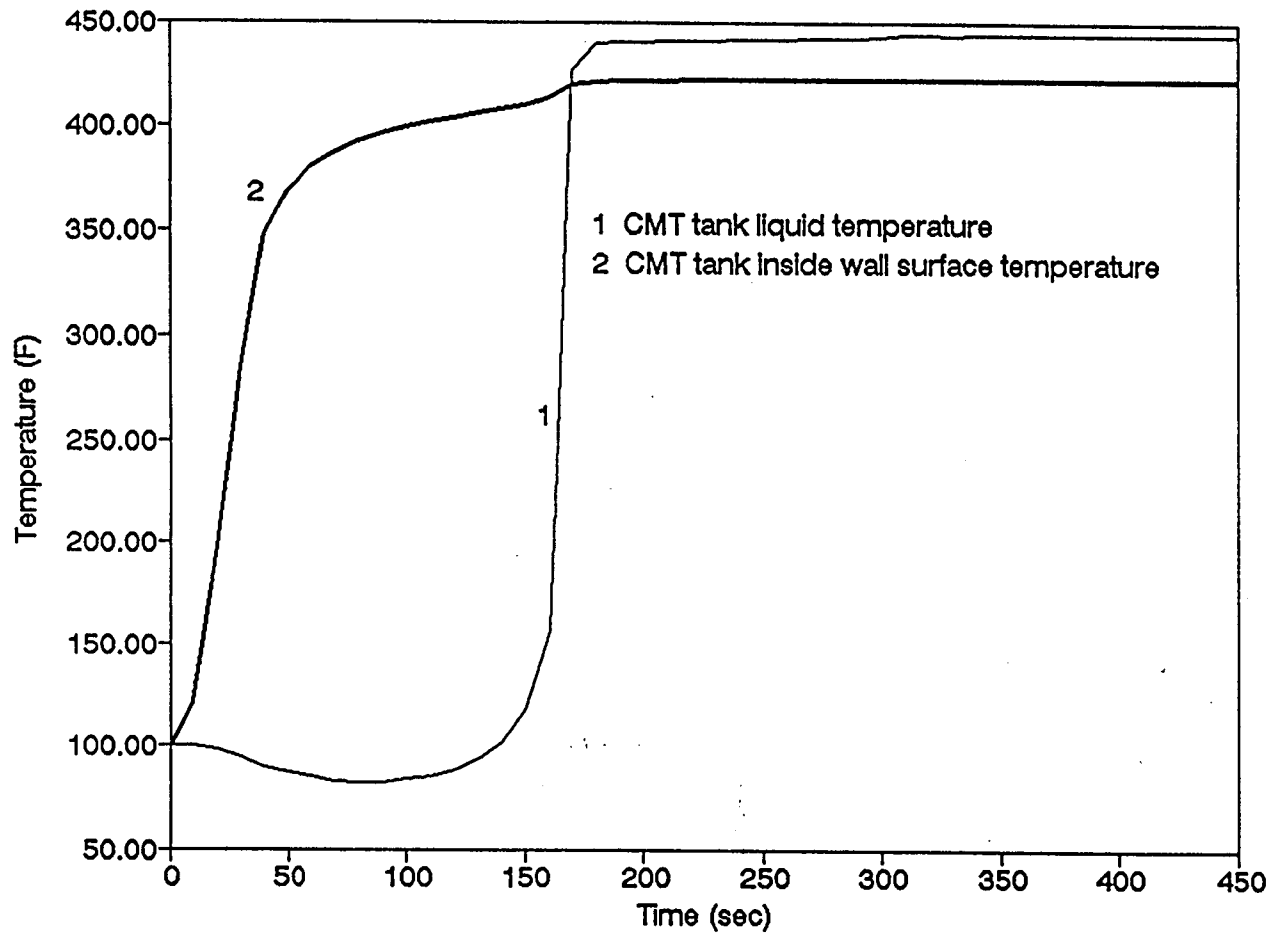


Figure 4.24 Comparison of temperatures between liquid volume and its adjoining heat structure

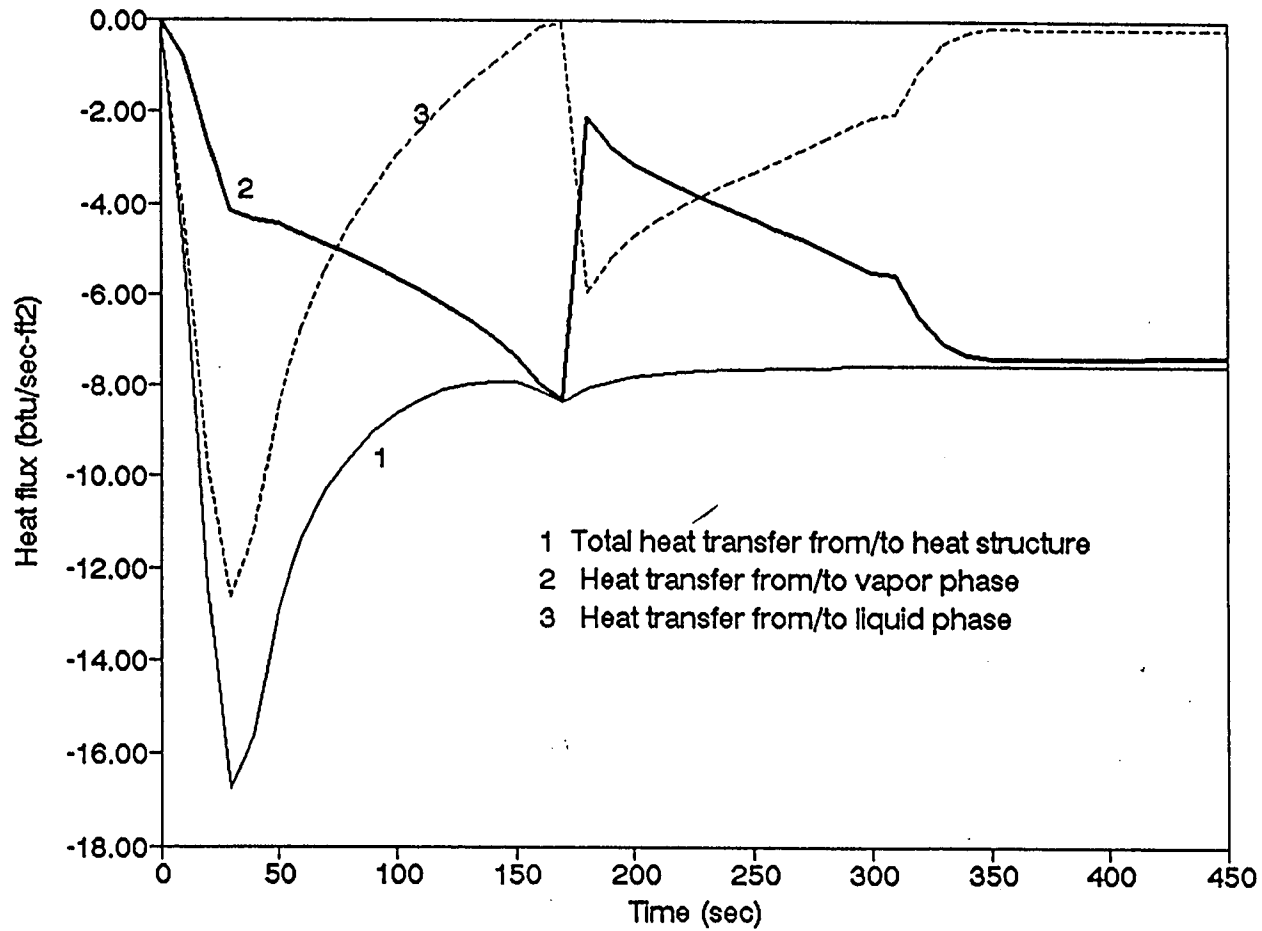


Figure 4.25 Comparison of heat flux between hydraulic volume and its adjoining heat structure

Appendices

Appendix A: Natural Convective Heat Transfer Coefficient For The Outer Surface of The CMT (OSU Model)

The main heat transfer mechanism of the heat loss from the Cmt to the surrounding is the natural convection (there is a possibility of radiation if you like to include). The heat transfer coefficient for the natural convection is governed by two nondimensionalized numbers. These numbers are:

1. Grashoff number which is given by:

$$GrL = K L^3(T_s - T_{air}) \quad \text{Grashoff number based on cylinder height.}$$

$$\text{where } K = \rho^2 g \beta / \mu^2$$

2. Prandtl number which is given by:

$$Pr = c_p \mu / k$$

We consider the surrounding temperature is the room temperature (100 °F). Using the air properties at this temperature results in:

$$K = 2.1e+6 \text{ } 1/(F\text{-ft}^3)$$

$$Pr = 0.71$$

The multiplication of Gr and Pr is called Rayleigh number (Ra) and the natural convection heat transfer coefficient is given usually in terms of Ra as follows:

$$h = c Ra^m k L$$

where k is the air conductivity and c and m are empirical constants based on Ra values as follows:

$$c = 0.59 \quad m = 0.25 \quad \text{for } 10^4 < Ra < 10^9 \quad (\text{Laminar}) [11]$$

$$c = 0.13 \quad m = 0.34 \quad \text{for } 10^9 < Ra < 10^{12} \quad (\text{Turbulent})$$

$$h = c (1.5e6)^m k L^{3m-1} (T_s - T_{air})^m$$

Based on the last equation, a table of h against T_s can be generated.

Appendix B: RELAP5 Input Deck for The Model Without Heat Structure

```

=====
= CMT tank steam/water interface condensation analysis without heat structure
=====
100 new transnt
101 run
102 british british
105 5. 10. 500.
201 100. 0.0000001 0.01 15003 100 10000 400
202 900. 0.0000001 0.1 15003 100 10000 400
=====
* minor edit variables
=====
302 mflowj 906000000
303 mflowj 861000000
310 vapgen 860010000
311 vapgen 860020000
312 vapgen 860030000
319 p 860010000
320 p 860020000
321 p 860030000
328 voidg 860010000
329 voidg 860020000
330 voidg 860030000
346 tempf 860010000
347 tempf 860020000
348 tempf 860030000
370 cntrivar 860
380 cntrivar 200
=====
* trip
=====
563 time 0 gt null 0 -1. 1 0
***** JUNCTION 855 *****
* cmt1-cold leg PBL valve
=====
8550000 cmt-inv valve
*
*   from   to   area   Kf   Kr   fvcahs
8550101 858050002 860010001 0.0000 0.00 0.00 000100
*   sc coeff 2p coeff sh coeff
8550102 1.00 1.00 1.00
*   hyd dia beta y-int slope
8550110 0.0000 0.00 1.00 1.00
*   vel/flow liquid vapor int-face
8550201 1 0.00 0.00 0.00
*   type
8550300 trpviv
*   trip
8550301 563
*
***** VOLUME 857 *****
* cmt1-cold leg pressure balance line
=====
8570000 cmt1-cl pipe
=====

```

```

*      no. vols
8570001  7
*      vol area
8570101  0.0068  1
8570102  0.0068  7
*      jun area
8570201  0.0068  6
*      length
8570301  1.4500  3
8570302  1.5420  4
8570303  1.6420  5
8570304  1.4400  7
*      volume
8570401  0.0000  7
*      azim angle
8570501  0.0000  7
*      incl angle
8570601  90.0000  3
8570602  0.0000  4
8570603  44.0000  7
*      delta z
8570701  1.4500  3
8570702  0.0000  4
8570703  0.2000  5
8570704  0.1650  7
*      roughness hyd dia
8570801  0.00015  0.0933  7
*      Kf      Kr
8570901  0.0000  0.0000  2
8570902  0.9000  0.9000  3
8570903  0.0000  0.0000  4
8570904  0.9000  0.9000  5
8570905  0.0000  0.0000  6
*      pvbfe
8571001  00000  7
*      fvcchs
8571101  000000  6
*      ebt
8571201  002    400.00  1.00    0.00  0.00  0.00  7
*      vel/flow
8571300  1
*      liquid vapor int-face
8571301  0.00  0.00  0.00  6
*      hyd dia beta y-int slope
8571401  0.0933  0.00  1.00  1.00  6
*
***** VOLUME 858 *****
* cmt1-cold leg pressure balance line
*-----*
8580000  cmt1bal pipe
*-----*
*      no. vols
8580001  5
*      vol area
8580101  0.0068  5
*      jun area
8580201  0.0068  4
*      length
8580301  2.5966  4
8580302  0.5500  5
*      volume
8580401  0.0000  5

```

```

*      azim angle
8580501 0.0000 5
*      incl angle
8580601 0.0000 1
8580602 90.0000 2
8580603 44.0000 3
8580604 0.0000 4
8580605 -90.0000 5
*      delta z
8580701 0.0000 1
8580702 1.7800 2
8580703 0.5500 3
8580704 0.0000 4
8580705 -0.550 5
*      roughness hyd dia
8580801 0.00015 0.0933 5
*      Kf      Kr
8580901 0.7000 0.7000 4
*      pvbfe
8581001 00000 5
*      fvcchs
8581101 000000 4
*      ebt
8581201 002 400.00 1.00 0.00 0.00 0.00 5
*      vel/flow
8581300 1
*      liquid vapor int-face
8581301 0.00 0.00 0.00 4
*      hyd dia beta y-int slope
8581401 0.0933 0.00 1.00 1.00 4
*
***** VOLUME 860 *****
* core makeup tank 1
*-----*
8600000 cmt1 pipe
*-----*
*      no. vols
8600001 3
*      vol area
8600101 2.5349 2
8600102 0.0000 3
*      jun area
8600201 2.5349 2
*      length
8600301 2.5177 1
8600302 1.3800 2
8600303 0.8724 3
*      volume
8600401 0.0000 2
8600402 1.3907 3
*      azim angle
8600501 0.0000 3
*      incl angle
8600601 -90.0000 3
*      delta z
8600701 -2.5177 1
8600702 -1.3800 2
8600703 -0.8724 3
*      roughness hyd dia
8600801 0.00015 1.7970 2
8600802 0.00015 0.0000 3
*      Kf      Kr

```

```

8600901 0.0000 0.0000 2
*   pvbfe
8601001 00000 3
*   fvcahs
8601101 000000 2
*   ebt
8601201 003 400.00 100.00 0.00 0.00 0.00 3
*   vel/flow
8601300 1
*   liquid vapor int-face
8601301 0.00 0.00 0.00 2
*   hyd dia beta y-int slope
8601401 1.7970 0.00 1.00 1.00 1
8601402 0.0000 0.00 1.00 1.00 2
*
***** JUNCTION 861 *****
* cmt1-out valve
*-----*
8610000 cmt1out valve
*-----*
*   from to area Kf Kr fvcahs
8610101 860030002 862010001 0.0000 0.00 0.00 000100
*   sc coeff 2p coeff sh coeff
8610102 1.00 1.00 1.00
*   hyd dia beta y-int slope
8610110 0.0000 0.00 1.00 1.00
*   vel/flow liquid vapor int-face
8610201 1 0.00 0.00 0.00
*   type
8610300 trpviv
*   trip
8610301 563
*
***** VOLUME 862 *****
* cmt #1 injection line
*-----*
8620000 cmtline pipe
*-----*
*   no. vols
8620001 2
*   vol area
8620101 0.0068 2
*   jun area
8620201 0.0068 1
*   length
8620301 9.9460 2
*   volume
8620401 0.0000 2
*   azim angle
8620501 0.0000 2
*   incl angle
8620601 -90.0000 1
8620602 0.0000 2
*   delta z
8620701 -3.385 1
8620702 0.0000 2
*   roughness hyd dia
8620801 0.00015 0.0933 2
*   Kf Kr
8620901 3.0349 3.0300 1
*   pvbfe
8621001 00000 2

```

```

*      fvcahs
8621101 000000 1
*      ebt
8621201 003      400.00 100.00 0.00 0.00 0.00 2
*      vel/flow
8621300 1
*      liquid vapor int-face
8621301 0.00 0.00 0.00 1
*      hyd dia beta y-int slope
8621401 0.0933 0.00 1.00 1.00 1
*
***** JUNCTION 863 *****
* cmt1 isolation valve
*-----*
8630000 cmtliso valve
*-----*
*      from to area Kf Kr fvcahs
8630101 862020002 864010001 0.0000 0.00 0.00 000100
*      sc coeff 2p coeff sh coeff
8630102 1.00 1.00 1.00
*      hyd dia beta y-int slope
8630110 0.0000 0.00 1.00 1.00
*      vel/flow liquid vapor int-face
8630201 1 0.00 0.00 0.00
*      type
8630300 trpviv
*      trip
8630301 563
*
***** VOLUME 864 *****
* PSIS Line #1
*-----*
8640000 ecc1ln pipe
*-----*
*      no. vols
8640001 5
*      vol area
8640101 0.0068 2
8640102 0.0068 5
*      jun area
8640201 0.0068 1
8640202 0.0068 4
*      length
8640301 1.9114 5
*      volume
8640401 0.0000 5
*      azim angle
8640501 0.0000 5
*      incl angle
8640601 0.0000 5
*      delta z
8640701 0.0000 5
*      roughness hyd dia
8640801 0.00015 0.0933 5
*      Kf Kr
8640901 0.0000 0.0000 4
*      pvbfe
8641001 00000 5
*      fvcahs
8641101 000000 4
*      ebt
8641201 003      400.00 100.00 0.00 0.00 0.00 5

```

```

*   vel/flow
8641300 1
*   liquid vapor int-face
8641301 0.00 0.00 0.00 4
*   hyd dia beta y-int slope
8641401 0.0933 0.00 1.00 1.00 4
*
***** VOLUME 900 *****
* entrance boundary volume
=====
9000000 sourcet snglvol
*-----*
*   area          length          volume
9000101 100000.0000 100000.0000 0.0000
*   azim angle          incl angle          delta z
9000102 0.00          0.00          0.0000
*   roughness          hyd dia          pvbfe
9000103 0.00015          0.0000          00010
*   ebt
9000200 002 400.00 1.00
*
***** JUNCTION 906 *****
* inlet junction
=====
9060000 inletj sngljun
*-----*
*   from to area Kf Kr fvcabs
9060101 900000000 857010001 0.0000 0.00 0.00 000100
*   sc coeff 2p coeff sh coeff
9060102 1.00 1.00 1.00
*   hyd dia beta y-int slope
9060110 0.0000 0.00 1.00 1.00
*   vel/flow liquid vapor int-face
9060201 1 0.00 0.00 0.00
*
***** JUNCTION 854 *****
* joint junction
=====
8540000 jointj sngljun
*-----*
8540101 857070002 858010001 0.0000 0.00 0.00 000000
8540102 1.00 1.00 1.00
8540110 0.0000 0.00 1.00 1.00
8540201 1 0.00 0.00 0.00
*
***** VOLUME 910 *****
* outlet boundary volume
=====
9100000 draint tmdpvol
*-----*
*   area          length          volume
9100101 100000.0000 100000.0000 0.0000
*   azim angle          incl angle          delta z
9100102 0.00          0.00          0.0000
*   roughness          hyd dia          pvbfe
9100103 0.00015          0.0000          00010
*   ebt trip search var
9100200 003 0
*   indep var
9100201 0.00 400.00 100.00
*
***** JUNCTION 915 *****

```

```

* outlet junction
*-----*
9150000 outletj sngljun
*-----*
*      from  to    area  Kf  Kr  fvcchs
9150101 864050002 910000000 0.0000  0.00  0.00  000100
*      sc coeff 2p coeff sh coeff
9150102 1.00  1.00  1.00
*      hyd dia  beta  y-int  slope
9150110 0.0000  0.00  1.00  1.00
*      vel/flow liquid vapor  int-face
9150201 1  0.00  0.00  0.00
*
***** CVAR 860 *****
* cmt tank water level
*-----*
*      name  type  factor  init value  init flag  limit min/max max
20586000 cmtlevel sum  1.00  4.7555  0  2  4.76
*-----*
20586001 0.0000  2.5177  voidf  860010000
20586002  1.3800  voidf  860020000
20586003  0.8724  voidf  860030000
*
***** CVAR 200 *****
* total injectin water through cmt tank outlet nozzle
*-----*
20520000 injectw  integral 2.2046  0.00  0  0
20520001 mflowj  861000000
*
/////end card

```

Appendix C: RELAP5 Input Deck for The Model With Heat Structure

```

=====
= CMT tank steam/water interface condensation analysis with heat structure
=====
100 new transnt
101 run
102 british british
105 5. 10. 500.
201 500. 0.0000001 0.1 1 100 100000 400
=====
* minor edit variables
=====
341 tempf 860010000
342 tempf 860020000
343 tempf 860030000
344 httemp 860100101
345 httemp 860100201
346 httemp 860100301
347 htrnr 860100100
348 htrnr 860100200
349 htrnr 860100300
350 htrg 860100100
351 htrg 860100200
352 htrg 860100300
=====
*trip
=====
563 time 0 gt null 0 -1. 1 0
***** JUNCTION 855 *****
* cmt1-cold leg PBL valve
=====
8550000 cmt-inv valve
=====
*
*   from   to   area   Kf   Kr   fvcahs
8550101 858050002 860010001 0.0000   0.00 0.00 000100
*   sc coeff 2p coeff sh coeff
8550102 1.00   1.00   1.00
*   hyd dia  beta   y-int  slope
8550110 0.0000 0.00   1.00   1.00
*   vel/flow liquid vapor  int-face
8550201 1     0.00  0.00   0.00
*   type
8550300 trpvlv
*   trip
8550301 563
*
***** VOLUME 857 *****
* cmt1-cold leg pressure balance line
=====
8570000 cmt1-cl pipe
=====
*   no. vols
8570001 7
*   vol area

```

```

8570101 0.0068 1
8570102 0.0068 7
*   jun area
8570201 0.0068 6
*   length
8570301 1.4500 3
8570302 1.5420 4
8570303 1.6420 5
8570304 1.4400 7
*   volume
8570401 0.0000 7
*   azim angle
8570501 0.0000 7
*   incl angle
8570601 90.0000 3
8570602 0.0000 4
8570603 44.0000 7
*   delta z
8570701 1.4500 3
8570702 0.0000 4
8570703 0.2000 5
8570704 0.1650 7
*   roughness hyd dia
8570801 0.00015 0.0933 7
*   Kf   Kr
8570901 0.0000 0.0000 2
8570902 0.9000 0.9000 3
8570903 0.0000 0.0000 4
8570904 0.9000 0.9000 5
8570905 0.0000 0.0000 6
*   pvbfe
8571001 00000 7
*   fvcahs
8571101 000000 6
*   ebt
8571201 002 400.00 1.00 0.00 0.00 0.00 7
*   vel/flow
8571300 1
*   liquid vapor int-face
8571301 0.00 0.00 0.00 6
*   hyd dia beta y-int slope
8571401 0.0933 0.00 1.00 1.00 6
*
***** VOLUME 858 *****
* cmt1-cold leg pressure balance line
*-----*
8580000 cmt1bal pipe
*-----*
*   no. vols
8580001 5
*   vol area
8580101 0.0068 5
*   jun area
8580201 0.0068 4
*   length
8580301 2.5966 4
8580302 0.5500 5
*   volume
8580401 0.0000 5
*   azim angle
8580501 0.0000 5
*   incl angle

```

```

8580601 0.0000 1
8580602 90.0000 2
8580603 44.0000 3
8580604 0.0000 4
8580605 -90.0000 5
*   delta z
8580701 0.0000 1
8580702 1.7800 2
8580703 0.5500 3
8580704 0.0000 4
8580705 -0.550 5
*   roughness hyd dia
8580801 0.00015 0.0933 5
*   Kf   Kr
8580901 0.7000 0.7000 4
*   pvbfe
8581001 00000 5
*   fvcchs
8581101 000000 4
*   ebt
8581201 002 400.00 1.00 0.00 0.00 0.00 5
*   vel/flow
8581300 1
*   liquid vapor int-face
8581301 0.00 0.00 0.00 4
*   hyd dia beta y-int slope
8581401 0.0933 0.00 1.00 1.00 4
*
***** VOLUME 860 *****
* core makeup tank 1
*-----*
8600000 cmt1 pipe
*-----*
*   no. vols
8600001 3
*   vol area
8600101 2.5349 2
8600102 0.0000 3
*   jun area
8600201 2.5349 2
*   length
8600301 2.1800 1
8600302 1.7164 2
8600303 0.8724 3
*   volume
8600401 0.0000 2
8600402 1.3907 3
*   azim angle
8600501 0.0000 3
*   incl angle
8600601 -90.0000 3
*   delta z
8600701 -2.1800 1
8600702 -1.7164 2
8600703 -0.8724 3
*   roughness hyd dia
8600801 0.00015 1.7970 2
8600802 0.00015 0.0000 3
*   Kf   Kr
8600901 0.0000 0.0000 2
*   pvbfe
8601001 00000 3

```

```

*      fvcahs
8601101 000000 2
*      ebt
8601201 003      400.00  100.00  0.00  0.00  0.00  3
*      vel/flow
8601300 1
*      liquid  vapor  int-face
8601301 0.00  0.00  0.00  2
*      hyd dia  beta  y-int  slope
8601401 1.7970  0.00  1.00  1.00  1
8601402 0.0000  0.00  1.00  1.00  2
*
***** JUNCTION 861 *****
* cmt1-out valve
=====
8610000 cmt1out valve
=====
*      from  to  area  Kf  Kr  fvcahs
8610101 860030002 862010001 0.0000  0.00  0.00  000100
*      sc coeff 2p coeff sh coeff
8610102 1.00  1.00  1.00
*      hyd dia  beta  y-int  slope
8610110 0.0000  0.00  1.00  1.00
*      vel/flow liquid  vapor  int-face
8610201 1      0.00  0.00  0.00
*      type
8610300 trpvlv
*      trip
8610301 563
*
***** VOLUME 862 *****
* cmt #1 injection line
=====
8620000 cmtline pipe
=====
*      no. vols
8620001 2
*      vol area
8620101 0.0068 2
*      jun area
8620201 0.0068 1
*      length
8620301 9.9460 2
*      volume
8620401 0.0000 2
*      azim angle
8620501 0.0000 2
*      incl angle
8620601 -90.0000 1
8620602 0.0000 2
*      delta z
8620701 -3.385 1
8620702 0.0000 2
*      roughness hyd dia
8620801 0.00015 0.0933 2
*      Kf  Kr
8620901 3.0349 3.0300 1
*      pvbfe
8621001 00000 2
*      fvcahs
8621101 000000 1
*      ebt

```

8621201 003 400.00 100.00 0.00 0.00 0.00 2

* vel/flow

8621300 1

* liquid vapor int-face

8621301 0.00 0.00 0.00 1

* hyd dia beta y-int slope

8621401 0.0933 0.00 1.00 1.00 1

*

***** JUNCTION 863 *****

* cmt1 isolation valve

8630000 cmtliso valve

-----*

* from to area Kf Kr fvcahs

8630101 862020002 864010001 0.0000 0.00 0.00 000100

* sc coeff 2p coeff sh coeff

8630102 1.00 1.00 1.00

* hyd dia beta y-int slope

8630110 0.0000 0.00 1.00 1.00

* vel/flow liquid vapor int-face

8630201 1 0.00 0.00 0.00

* type

8630300 trpvlv

* trip

8630301 563

*

***** VOLUME 864 *****

* PSIS Line #1

8640000 ecc1ln pipe

-----*

* no. vols

8640001 5

* vol area

8640101 0.0068 2

8640102 0.0068 5

* jun area

8640201 0.0068 1

8640202 0.0068 4

* length

8640301 1.9114 5

* volume

8640401 0.0000 5

* azim angle

8640501 0.0000 5

* incl angle

8640601 0.0000 5

* delta z

8640701 0.0000 5

* roughness hyd dia

8640801 0.00015 0.0933 5

* Kf Kr

8640901 0.0000 0.0000 4

* pvbfe

8641001 00000 5

* fvcahs

8641101 000000 4

* ebt

8641201 003 400.00 100.00 0.00 0.00 0.00 5

* vel/flow

8641300 1

* liquid vapor int-face

```

8641301 0.00 0.00 0.00 4
*   hyd dia  beta  y-int  slope
8641401 0.0933 0.00 1.00 1.00 4
*
***** VOLUME 900 *****
* entrance boundary volume
*****
9000000 sourcet  snglvol
*-----*
*   area          length          volume
9000101 100000.0000  100000.0000  0.0000
*   azim angle          incl angle          delta z
9000102 0.00          0.00          0.0000
*   roughness          hyd dia          pvbfe
9000103 0.00015          0.0000          00010
*   ebt
9000200 002  400.00  1.00
*
***** JUNCTION 906 *****
* inlet junction
*****
9060000 inletj  sngljun
*-----*
*   from  to  area  Kf  Kr  fvcahs
9060101 9000000000 857010001 0.0000  0.00  0.00  000100
*   sc coeff 2p coeff sh coeff
9060102 1.00  1.00  1.00
*   hyd dia  beta  y-int  slope
9060110 0.0000  0.00  1.00  1.00
*   vel/flow liquid vapor  int-face
9060201 1  0.00  0.00  0.00
*
***** JUNCTION 854 *****
* joint junction
*****
8540000 jointj  sngljun
*-----p 1-----*
8540101 857070002 858010001 0.0000  0.00  0.00  000000
8540102 1.00  1.00  1.00
8540110 0.0000  0.00  1.00  1.00
8540201 1  0.00  0.00  0.00
*
***** VOLUME 910 *****
* outlet boundary volume
*****
9100000 draint  tndpvol
*-----*
*   area          length          volume
9100101 100000.0000  100000.0000  0.0000
*   azim angle          incl angle          delta z
9100102 0.00          0.00          0.0000
*   roughness          hyd dia          pvbfe
9100103 0.00015          0.0000          00010
*   ebt  trip  search var
9100200 003  0
*   indep var
9100201 0.00  400.00  100.00
*
***** JUNCTION 915 *****
* outlet junction
*****
9150000 outletj  sngljun

```

```

*-----*
*   from   to   area   Kf   Kr   fvcchs
9150101 864050002 910000000 0.0000   0.00  0.00  000100
*   sc coeff 2p coeff sh coeff
9150102 1.00   1.00   1.00
*   hyd dia  beta   y-int  slope
9150110 0.0000  0.00   1.00   1.00
*   vel/flow liquid vapor   int-face
9150201 1     0.00   0.00   0.00
*
***** STRUCTURE 8601 *****
* cylindrical part of CMT tank
*-----*
*   no. str  m.pts  geom   init flag  l-coord  reflood bvol-i ax-int
18601000 3     6     2 0     0.8985 0
*-----*
*   loc flag form flag
18601100 0     2
*   mesh int  int no.
18601101 0.0203  1
18601102 0.0203  2
18601103 0.0203  3
18601104 0.0203  4
18601105 0.0203  5
*   compos no.      int no.
18601201 7     1
18601202 7     2
18601203 7     3
18601204 7     4
18601205 7     5
*   source val      int no.
18601301 0.0000  1
18601302 0.0000  2
18601303 0.0000  3
18601304 0.0000  4
18601305 0.0000  5
*   init temp
18601400 0
*   temp   m-pt no.
18601401 100.00  1
18601402 100.00  2
18601403 100.00  3
18601404 100.00  4
18601405 100.00  5
18601406 100.00  6
*   b-vol/tab incr  bc-type  sa-code sa/factor  hs no.
18601501 860010000 0     1 1     2.1800 1
18601502 860020000 0     1 1     1.7164 2
18601503 860030000 0     1 1     0.8724 3
*   b-vol/tab incr  bc-type  sa-code sa/factor  hs no.
18601601 -100   0     4400 1     2.1800 1
18601602 -100   0     4400 1     1.7164 2
18601603 -100   0     4400 1     0.8724 3
*   srce-type mult  dhmult-l  dhmult-r  hs no.
18601701 0     0.000  0.000  0.000  1
18601702 0     0.000  0.000  0.000  2
18601703 0     0.000  0.000  0.000  3
*   Dhe   heatle-f heatle-r  sple-f sple-r  gr-Kf gr-Kr  local-BF hs no.
18601801 0.0000  10.00  10.00  0.00  0.00  0.00  0.00  1.00 1
18601802 0.0000  10.00  10.00  0.00  0.00  0.00  0.00  1.00 2
18601803 0.0000  10.00  10.00  0.00  0.00  0.00  0.00  1.00 3
*   Dhe   heatle-f heatle-r  sple-f sple-r  gr-Kf gr-Kr  local-BF hs no.

```

18601901 0.0000 10.00 10.00 0.00 0.00 0.00 0.00 1.00 1
 18601902 0.0000 10.00 10.00 0.00 0.00 0.00 0.00 1.00 2
 18601903 0.0000 10.00 10.00 0.00 0.00 0.00 0.00 1.00 3

*
 ***** COMPOSITION 7 *****

* stainless steel

=====*

* mat type

20100700 tbl/fctn 1 1

*
 * Thermal conductivity table

20100701 32. 0.002083

20100702 1700. 0.004029

*
 * Volumetric heat capacity table

20100751 68. 53.6800

20100752 200. 57.1100

20100753 300. 59.1200

20100754 400. 61.1200

20100755 500. 63.1300

*
 ***** TABLE 100 *****

* enviromental temperature

=====*

* type trip factor factor factor

20210000 temp 0 1.00 1.00 0.00

=====*

* arg value func value

20210001 0.00 100.00

20210002 100000.00 100.00

*
 ***** TABLE 400 *****

* HT coefficient for cylindrical part

=====*

* type trip factor factor factor

20240000 htc-temp 0 1.00 0.00 1.00

=====*

* arg value func value

20240001 100.00 0.00

20240002 110.00 0.43

20240003 150.00 0.98

20240004 200.00 1.24

20240005 250.00 1.42

20240006 300.00 1.57

20240007 350.00 1.69

20240008 400.00 1.80

20240009 450.00 1.90

*
 ***** CVAR 860 *****

* cmt tank water level

=====*

* name type factor init value init flag limit min/max max

20586000 cmtlevel sum 1.00 4.7555 0 2 4.76

=====*

20586001 0.0000 2.1800 voidf 860010000

20586002 1.7164 voidf 860020000

20586003 0.8724 voidf 860030000

*
 /////end card